

Contrasting transit times of water from peatlands and eucalypt forests in the Australian Alps determined by tritium: implications for vulnerability and the source of water in upland catchments

5 **Ian Cartwright^{1,2} and Uwe Morgenstern³**

¹*School of Earth, Atmosphere and Environment, Monash University, Clayton, Vic. 3800, Australia*

10 ²*National Centre for Groundwater Research and Training, GPO box 2100, Flinders University, Adelaide, SA 5001, Australia*

³*GNS Science, Lower Hutt 5040, New Zealand*

Correspondence to: I. Cartwright (ian.cartwright@monash.edu)

Abstract

Peatlands are a distinctive and important component of many upland regions that commonly contain distinctive flora and fauna which are different from those of adjacent forests and grasslands. Peatlands also represent a significant long-term store of organic carbon. While their environmental importance

5 has long since been recognised, water transit times within peatlands are not well understood. This study uses tritium (${}^3\text{H}$) to estimate the mean transit times of water from peatlands and from adjacent gullies that contain eucalypt forests in the Victorian Alps (Australia). The ${}^3\text{H}$ activities of the peatland water range from 2.7 to 3.3 Tritium Units (TU), which overlap the measured (2.9 to 3.0 TU) and expected (2.8 to 3.2 TU) average ${}^3\text{H}$ activities of rainfall in this region. Even accounting for seasonal
10 recharge by rainfall with higher ${}^3\text{H}$ activities, the mean transit times of the peatland waters are <6.5 years and may be less than 2 years. Water from adjacent eucalypt forest streams has ${}^3\text{H}$ activities of 1.6 to 2.1 TU, implying much longer mean transit times of 5 to 29 years. Cation/Cl and Si/Cl ratios are higher in the eucalypt forest streams than the peatland waters and both of these water stores have higher cation/Cl and Si/Cl ratios than rainfall. The major ion geochemistry reflects the degree of silicate
15 weathering in these catchments that is controlled by both transit times and aquifer lithology. The short transit times imply that, unlike the eucalypt forests, the peatlands do not represent a long-lived store of water for the local river systems. Additionally, the peatlands are susceptible to drying out during drought which renders them vulnerable to damage by the periodic bushfires that occur in this region.

1. Introduction

Globally, peatlands occupy parts of the upland areas of many river catchments and provide water to the headwater streams in those catchments. It is estimated that peatlands cover $\sim 4 \times 10^6 \text{ km}^2$ or $\sim 3\%$ of the world's land area (Dixon et al., 1994). Peatlands have received much attention because they

5 represent a major (1.8 to 4.5×10^{11} tonne) long-lived store of terrestrial organic carbon (Gorham, 1991; Page et al., 2002). Peatlands commonly contain distinctive flora such as sphagnum moss, sedges, and orchids that may not occur in surrounding forests or grasslands (Grover and Baldock, 2013; Grover et al., 2005; McDougall, 1982). Due to their unique flora, there may be also differences in fauna between the peatlands and the surrounding regions.

10 Draining of peatlands is a major environmental concern. This can occur directly due to anthropogenic activities such as peat extraction and the conversion of peatland to agricultural land or forest. Additionally, since peatlands form in high rainfall environments, drainage can occur due to a reduction in rainfall. Draining of peatlands destroys the habitats of flora and fauna and also causes oxidation of the organic matter, which in turn releases CO_2 to the atmosphere (Gorham, 1991; Grover and Baldock, 15 2010). In addition, the dried peat is susceptible to bushfires that commonly occur during droughts and which can destroy the peatlands (Van Der Werf et al., 2010).

Peatlands comprise $\sim 520 \text{ km}^2$ or $\sim 2.5\%$ of the alpine region of the southeast Australian mainland (Fig. 1) (Costin, 1972; Grover et al., 2005; Western et al., 2009). The peat generally occupies shallowly-sloping areas in the upland plains that are poorly drained. While it forms only a minor part of the 20 Australian landscape, understanding the water balance in the Australian peatlands is important for assessing the potential impacts of environmental change. If water transit times are short, then the peatlands may dry significantly during droughts making them prone to degradation and vulnerable to bushfires. Additionally, the peatlands provide water to numerous small upland streams. Most of the upland peatlands are flanked by eucalypt forests that occupy steeper slopes and gullies. Eucalypts 25 have high transpiration rates and groundwater recharge rates in eucalypt-dominated areas are low (Allison et al., 1990), which results in relatively long water transit times (on the order of years to decades) in eucalypt-dominated catchments (Cartwright and Morgenstern, 2015).

1.1 Determining mean transit times

The mean transit time represents the average time required for water to flow through the aquifer or soil from where it recharges to where it discharges at the surface (e.g., at a spring, stream or lake) or is sampled from a bore (Cook and Bohlke, 2000; Maloszewski and Zuber, 1982; McDonnell et al., 2010).

5 Documenting mean transit times is important for understanding and managing catchments. The time required for nutrients or contaminants to be transported from recharge areas to streams is a direct function of the transit time (Morgenstern and Daughney, 2012). Additionally, catchments with long transit times are more likely to be resilient to short-term (years to decades) variations in rainfall but will respond to climate or landuse changes that cause longer-term (decades to centuries) changes in
10 groundwater recharge and flow.

Tritium (^3H) has a half-life of 12.32 yr which, together with the fact that it is part of the water molecule, makes it an ideal tracer for determining transit times of young shallow groundwater, soil water, or surface water (Clark and Frtiz, 1997; Cook and Bohlke, 2000; Morgenstern et al., 2010). Other potential tracers for determining transit times of young waters, such as ^3He , chlorofluorocarbons, and SF_6 are

15 gases that degas to the atmosphere and are thus difficult to use for water sampled from streams. Because the seasonal variation of stable isotope ratios or major ion concentrations in recharge is attenuated with increasing transit times, time-series of stable isotope ratios or Cl concentrations are also commonly used to estimate mean transit times (e.g., McGuire and McDonnell, 2006; Hrachowitz et al., 2010, 2013; Kirchner et al., 2010). However, this is only practicable where mean transit times
20 are shorter than ~5 years, as longer transit times attenuates the seasonal variation of these tracers (Stewart et al., 2010). Additionally, the use of these tracers requires a detailed (preferably at least weekly) record of stable isotope and/or major ion geochemistry in rainfall for a period which exceeds that of the transit times of water in the catchment (e.g. Timbe et al., 2015).

Coupled with models that describe the distribution of flow paths within an aquifer, commonly referred
25 to as lumped parameter models (Cook and Bohlke, 2000; Maloszewski, 2000; McGuire and McDonnell, 2006), ^3H may be used to determine transit times of waters that are up to ~100 years old. The ^3H activities in rainfall over the last several decades have been measured globally (e.g. International Atomic Energy Association, 2016; Tadros et al., 2014), which allows the ^3H input to catchments over

time to be estimated. Rainfall ${}^3\text{H}$ activities peaked in the 1950s to 1960s due to the production of ${}^3\text{H}$ in atmospheric thermonuclear tests (commonly termed “bomb pulse” ${}^3\text{H}$).

There are two different approaches in using ${}^3\text{H}$ to estimate mean transit times. In the northern hemisphere, the ${}^3\text{H}$ activities of remnant bomb pulse waters are currently above those of modern

5 rainfall. This situation results in individual measurements of ${}^3\text{H}$ activities in groundwater or surface water yielding non-unique estimates of transit times (Morgenstern et al., 2010). Mean transit times may, however, be determined using time-series of ${}^3\text{H}$ measurements (e.g., Maloszewski and Zuber, 1982; Michel, 1992, McGuire and McDonnell, 2006). The use of time-series measurements is potentially advantageous as, in addition to determining a mean transit time, it allows the most 10 appropriate lumped parameter model to be assessed by comparison of the predicted and observed changes to ${}^3\text{H}$ activities over time (Maloszewski and Zuber, 1982). However, constraining lumped parameter models using sequential ${}^3\text{H}$ data collected over several years has commonly made the assumption that the data can be described by a single lumped parameter model and that the flow system is time invariant, which may not be the case in reality (e.g., Kirchner, 2016b).

15 The bomb pulse ${}^3\text{H}$ activities in the southern hemisphere were several orders of magnitude lower than in the northern hemisphere (Clark and Fritz, 1997; Tadros et al., 2014) and the ${}^3\text{H}$ activities of the remnant bomb-pulse waters have now decayed below those of modern rainfall. This permits ${}^3\text{H}$ to be used in a similar manner to other radioactive isotope tracers such as ${}^{14}\text{C}$ or ${}^{36}\text{C}$ whereby a residence or transit time may be estimated from individual ${}^3\text{H}$ activities (Morgenstern et al., 2010). Since the ${}^3\text{H}$ 20 activities reflect the net residence time in the catchment there is not a requirement for the flow system to be time invariant. However, this approach to determining mean transit times does not permit the optimal lumped parameter model to be determined, as is the case when time-series ${}^3\text{H}$ measurements at similar flow conditions are available. The attenuation of the bomb-pulse ${}^3\text{H}$ in the southern hemisphere is such that constraining the lumped parameter models using time-series 25 measurements of ${}^3\text{H}$ is probably no longer practicable. For example, the predicted decrease in ${}^3\text{H}$ activities for a water with a mean transit time of 10 years between 2016 and 2026 calculated using the lumped parameter models and ${}^3\text{H}$ input employed in this study is only ~ 0.2 TU, and the predicted ${}^3\text{H}$ vs time trends are similar for the different models. Instead, a plausible lumped parameter model

must be proposed based on factors such as the geometry of the flow system or information from previous time-series studies. Given that the different lumped parameter models yield different mean transit times for the same ${}^3\text{H}$ activity, this introduces uncertainties. However, because the ${}^3\text{H}$ activities of the remnant bomb pulse waters are below those of modern rainfall, the relative transit times of 5 southern hemisphere waters are largely independent of assumed flow models (i.e., water with a low ${}^3\text{H}$ activity has a longer mean transit time than water with a high ${}^3\text{H}$ activity).

Rivers aggregate water from different flow systems and the mean transit times of water contributed by individual tributaries may vary considerably. Kirchner (2016a) discussed the impacts of aggregation for mean transit times calculated from time-series major ion and stable isotope data. That study 10 demonstrated that the mean transit time calculated from the aggregated water was generally lower than the actual mean transit time (i.e. that which would be calculated from the weighted average of each of the end-members contributing to the mixture). Aggregation also affects mean transit times calculated from individual ${}^3\text{H}$ activities. Mean transit times calculated from the ${}^3\text{H}$ activity of the aggregated water are again generally lower than the actual mean transit times with the error 15 increasing as the difference between the mean transit time of the individual end members increases (Stewart et al., 2016).

1.2 Transit times in upland peat

Compared with catchments developed on other vegetation types, the transit time of peatland water, especially upland or mountain peat, is less well known. Due to peatlands containing poorly-drained 20 organic rich soils and occupying shallow slopes, it is sometimes assumed that peatland waters have long transit times. However, there has been little assessment of that assumption (e.g., as discussed by Western et al., 2009). Using ${}^3\text{H}$ activities, transit times of years to decades were proposed for water from metre to tens-of-metre thick peat deposits in Quebec, Canada (Dever et al., 1984), Dartmoor, UK, (Charman et al., 1999), Lithuania (Mažeika et al., 2009), and Minnesota, USA (Siegel et al., 2001). 25 From the preservation of seasonal $\delta^{18}\text{O}$ and $\delta^2\text{H}$ values, Aravena and Warner (1992) estimated that the water from the upper ~ 0.1 m of peat from Ontario, Canada, was < 1 year old. Mean transit times from an upland peat-bearing catchment in Zhurucay, Ecuador, were estimated at < 1 year using oxygen isotopes (Mosquera et al., 2016). Mean transit times from the extensively-studied upland catchments

in the United Kingdom, which include extensive regions of peat, were estimated using time series of stable isotopes and Cl as <5 years (e.g., Soulsby et al., 2006; Kirchner et al., 2010; Hrachowitz et al., 2013; Tetzlaff et al., 2014, Benettin et al., 2015). However, the mean transit times of the water specifically draining the peat in those catchments are generally not known. Morris and Waddington 5 (2011) modelled water transit times in peat and suggested that they vary from <1 year for the upper 0.1 m to several years in deeper layers, which is broadly consistent with the above estimates. While not estimating transit times, Western et al. (2009) concluded on the basis of hydrograph analysis and water balance calculations that peatlands in southeast Australia did not act as long-term water stores for the local streams.

10 **1.3 Objectives**

This study was designed to test the hypothesis that peatlands in the Victorian Alps, southeast Australia represent a relatively long-lived store of water. Specifically, we utilise ^3H to provide the first estimates of the mean transit times of water draining Australian peatlands during summer baseflow conditions and compare these with mean transit times of streams that drain adjacent eucalypt forests. 15 Documenting mean transit times is important for determining the relative importance of the peatlands and eucalypt forests in providing water to the local rivers and also in assessing potential environmental impacts resulting from landuse or climate change. In addition, we assess whether the major ion geochemistry of the water may be used as a first-order proxy for mean transit times and discuss the controls on mean transit times in these upland areas.

20 **2. Methods**

2.1 Setting

Water from streams draining peatlands and eucalypt forests was sampled in the Mount Buffalo (Ovens Catchment: Fig. S1a), Falls Creek (Kiewa and Upper Murray Catchments: Fig. S1b), and Dargo (Mitchell Catchment: Fig. S1c) regions of the Victorian Alps (Fig. 1). Catchment areas in the peatlands and 25 eucalypt forests are similar, ranging from 0.5 to 6.4 km² (Table 1). The Falls Creek and Dargo areas consist of indurated Ordovician metasedimentary rocks, Devonian granites, and minor Tertiary basalts,

whereas the Mount Buffalo plateau comprises Devonian granite (van den Berg et al., 2004; Energy and Earth Resources, 2016).

Peatlands are developed in poorly-drained low-relief upland areas of the Victorian Alps with eucalyptus forests occupying steeper valleys that dissect the uplands and the higher better-drained 5 areas at the margins of the peatland (Grover and Baldock, 2013; Grover et al., 2005; McDougall, 1982; Western et al., 2009). The peatlands are characterised by sphagnum mosses (*Sphagnum cristatum*), rushes (*Empodisma minus* and *Baloskion australe*), and heaths (*Epacris paludosa* and *Richea continentis*) (McDougall, 1982). Most of the peatlands in the Alpine region are <2 m thick. The upper 10 few centimetres comprise little decomposed plant material (the fibric zone). The fibric zone grades downwards through the hemic zone (typically 50 cm to 1 m thick) where the soils are organic-rich, fiberous, with abundant discernible roots into a denser soil (the sapric zone) comprising mainly decomposed organic matter with clays and fragments of rock. The peat typically has a thin (<20 cm thick) layer of weathered rocks at its base but mainly overlies little-weathered basement rocks. The 15 hydrology of the peat comprises the upper acrotelm, which alternates between saturated and unsaturated as the water table rises and falls, and the lower permanently-saturated catotelm (e.g., Grover et al., 2005). The boundary between the acrotelm and catotelm is generally in the hemic zone.

In the alpine regions of southeast Australia the dominant eucalypt species include Mountain Ash (*Eucalyptus regnans*) at altitudes of <1000 m and Alpine Ash (*Eucalyptus delegatensis*) and Snow Gum (*Eucalyptus pauciflora*) at higher altitudes (McDougall, 1982). The soils of the eucalypt forests include 20 sandy lithosols; these are thin, well-drained, and poor in organic matter and largely occur on the upper slopes of the gullies and on the elevated areas surrounding the peatlands. In the centres of the gullies, the soils also include alpine humus loams that contain higher contents of organic matter and which are less well drained. The soils overlie weathered regolith that is a few tens-of-centimetres to a few metres thick. There are also minor deposits of colluvium and alluvium along the streams (Shugg, 1987). 25 Groundwater flow is restricted to the weathered zones and fractures in the granites and metasediments; the minor alluvial and colluvial sediments are more permeable but represent only a minor part of the landscape.

Average precipitation is 1250 mm yr^{-1} at Falls Creek, 1650 mm yr^{-1} at Mount Hotham (near Dargo), and 1790 mm yr^{-1} at Mount Buffalo (Bureau of Meteorology, 2016) (Fig. 1). Approximately 60 to 70% of precipitation occurs in the austral autumn to winter (May to September) with a proportion of the winter precipitation occurring as snow. February and March have the lowest precipitation (4 to 6% of the annual total in each month). No currently active river gauges exist in these upland areas and previous flow measurements were only from a few streams at Falls Creek (Department of Environment, Land, Water, and Planning, 2016). These limited records show that river flow varies seasonally with the majority of streamflow occurring in the winter months; however, flows persist over summer (Fig. 2a) and the streams generally do not record zero flows (Fig. 2b). Water from some of the peatlands at Falls Creek drains into the Rocky Valley Reservoir ($\sim 2.8 \times 10^7 \text{ m}^3$), which is used to provide water to the Falls Creek resort and the Kiewa Valley hydroelectric system. Water from some of the peatlands at Mount Buffalo feeds Lake Catani, which is an artificial recreational lake with a volume of $\sim 2 \times 10^6 \text{ m}^3$.

Mean transit times in the Ovens Valley which is dominated by eucalypt forests (Fig. 1) were estimated using ^3H as being between 4 and 30 years, with higher mean transit times recorded during summer low flow conditions (Cartwright and Morgenstern, 2015). That study focussed on the major tributaries to the Ovens River that had catchment areas between 6 and 435 km^2 , and the transit times in the upper reaches of the catchments where streamflow commences remains unknown. Additionally, it was not established whether there are differences between mean transit times for water draining the peatlands and the eucalypt forests in those upper catchments.

20 **2.2 Sampling and analytical techniques**

Samples of rainfall representing the total precipitation over periods of several weeks to months (Table 1) were collected from a rainfall collector at Mount Buffalo (Fig. 1). Grab samples of stream water from the peatlands and eucalypt forests were taken from flowing reaches. Water was also sampled from within the peat using a hand-operated siphon pump with a soft PVC inlet hose that was inserted into a rigid 5 cm diameter PVC piezometer with a $\sim 20 \text{ cm}$ screen pushed directly into the peat. The piezometer was inserted to the maximum possible extent (i.e., until resistance prevented it from being pushed deeper). Field observations indicated that this was at or close to the base of the peat and

within the hemic zone and catotelm. At least three bore volumes of water were extracted prior to sampling.

Tritium activities (Table 1) were measured on water samples that had been vacuum distilled and electrolytically enriched using liquid scintillation spectrometry (Quantulus ultra-low-level counters) at

5 Geological and Nuclear Sciences, New Zealand (Morgenstern and Taylor, 2009). The ${}^3\text{H}$ activities are expressed in tritium units (TU) where 1 TU represents a ${}^3\text{H}/{}^1\text{H}$ ratio of 1×10^{-18} . Enrichment of ${}^3\text{H}$ was by a factor of 95, which results in a detection limit of 0.02 TU, while the use of deuterium-calibration for each sample results in a 1% reproducibility of the tritium enrichment. Precision (1σ) is $\sim 1.8\%$ at 2 TU.

10 Major ion concentrations (Table 1) were measured at Monash University using a ThermoFinnigan ICP-OES (cations), ThermoFinnigan ICP-MS (Si), and a ThermoFischer ion chromatograph (anions). Samples for cation and Si analysis were filtered through 0.45 μm cellulose nitrate filters and acidified to pH <2 using double-distilled 16M HNO_3 . Samples for anion analysis were filtered but unacidified. The precision of the major ion concentrations determined by replicate analyses of samples is $\pm 2\%$ and the 15 accuracy as determined by analysis of certified water standards is $\pm 5\%$.

Stable isotope ratios of water (Table 1) were determined using a ThermoFinnigan DeltaPlus Advantage mass spectrometer at Monash University. A ThermoFinnigan Gas Bench was used for the ${}^{18}\text{O}$ analyses.

Waters were equilibrated with He- CO_2 at 32 °C for 24 to 48 hours and the gas subsequently analysed by continuous flow. A ThermoFinnigan H-Device was used for the ${}^2\text{H}$ analyses. H was produced from

20 water via reaction with Cr at 850 °C and analysed by dual-inlet measurement. Internal standards that have been calibrated using IAEA SMOW, GISP and SLAP standards were employed to normalise the $\delta^{18}\text{O}$ and $\delta^2\text{H}$ values (following Coplen, 1988). The $\delta^{18}\text{O}$ and $\delta^2\text{H}$ values are expressed in ‰ relative to V-SMOW with a precision (1σ) determined from replicate analyses of samples of $\pm 0.1\text{‰}$ ($\delta^{18}\text{O}$) and $\pm 1\text{‰}$ ($\delta^2\text{H}$). The deuterium (D) excess is defined as $\delta^2\text{H} - 8 \delta^{18}\text{O}$ (Clark and Fritz, 1999).

25 Catchment areas (Table 1) were estimated from Google Earth satellite images (Figs S1a to S1c) and 1:30,000 topographic map sheets on which the streams are clearly distinguished. Attempts to define

catchment areas using a digital elevation model (DEM) did not reproduce the drainage pattern in the peatlands due to the low topography relative to the DEM resolution.

2.3 Estimating mean transit times using ${}^3\text{H}$

Water flowing through aquifers or soils follows flow paths of varying length and thus the water discharging into streams or sampled from bores has a range of transit times (McGuire and McDonnell, 2006). Mean transit times were calculated using lumped parameter models (Maloszewski, 2000; Maloszewski and Zuber, 1982; Zuber et al., 2005) as implemented in the TracerLPM Excel workbook (Jurgens et al., 2012). For steady-state groundwater flow, the ${}^3\text{H}$ activity in water at the catchment outlet at the time of sampling ($C_o(t)$) may be estimated using the convolution integral:

$$C_o(t) = \int_0^{\infty} C_i(t-\tau) g(\tau) e^{-\lambda\tau} d\tau \quad (1),$$

In Eq. (1), C_i is the ${}^3\text{H}$ activity of recharge, τ is the transit time, $t-\tau$ is the time when water entered the catchment, λ is the ${}^3\text{H}$ decay constant (0.0563 yr^{-1}), and $g(\tau)$ is the response function that describes the distribution of transit times in the flow system.

As discussed above, the use of single ${}^3\text{H}$ activities to estimate mean transit times requires that a lumped parameter model be assigned. The following lumped parameter models were considered in this study: the exponential flow model; the exponential-piston flow model; and the dispersion model. Together these represent the most commonly used lumped parameter models in determining mean transit times (e.g. as reviewed by McGuire & McDonnell, 2006). In catchments where time-series data are available, these models generally reproduce the predicted variation in ${}^3\text{H}$ activities over time (e.g., Maloszewski and Zuber, 1982; Maloszewski et al. 1983; Zuber et al., 2005; Stewart et al. 2007; Morgenstern et al., 2015).

The exponential flow model predicts transit times in homogeneous unconfined aquifers of constant thickness with uniform recharge where water from the entire aquifer discharges to the stream or is sampled by a bore. Flow through aquifers where flow paths are the same length and no mixing occurs results in all water discharging to the stream at any given time having the same transit time and is

described by the piston flow model. Transit times in aquifers that have regions of both piston and exponential flow are described by the exponential-piston flow model, for which the response function is:

$$g(\tau) = 0 \quad \text{for } \tau < \tau_m(1-f) \quad (2a)$$

$$5 \quad g(\tau) = (f\tau_m)^{-1} e^{-\tau/f\tau_m + 1/f - 1} \quad \text{for } \tau > \tau_m(1-f) \quad (2b),$$

where τ_m is the mean transit time and f is the proportion of the aquifer volume that exhibits exponential flow. At $f = 1$, this model becomes the exponential flow model, while at $f = 0$, it becomes the piston flow model. TracerLPM specifies the ratio of exponential to piston flow as the EPM ratio (equivalent to $1/f - 1$).

10 The dispersion model is based on the solution to the one-dimensional advection-dispersion transport equation. The response function for the dispersion model is:

$$g(\tau) = \frac{1}{\tau \sqrt{4\pi D_p \tau / \tau_m}} e^{-\left(\frac{(1-\tau/\tau_m)^2}{4D_p \tau / \tau_m}\right)} \quad (3),$$

where D_p is the dispersion parameter defined as $D_p = D/(v x)$, where D is the dispersion coefficient ($\text{m}^2 \text{ day}^{-1}$), v is velocity (m day^{-1}) and x is distance (m). This model is generally considered to be a less

15 realistic representation of flow systems, however it does commonly reproduce the observed distribution of tracers (Maloszewski, 2000).

In this study mean transit times were calculated by matching the predicted ${}^3\text{H}$ from the lumped parameter model to the measured value at the time of collection using TracerLPM. For these calculations, the form of the lumped parameter model and its parameters (i.e. the EPM ratio or D_p)
20 and the ${}^3\text{H}$ input function were specified.

3. Results

This section presents the streamflow and geochemistry data (Table 1) from the Victorian Alps; interpretation of these data appears in later sections.

3.1 Streamflow

As noted above, very few streamflow measurements exists in these catchments. Watchbed Creek drains the peatlands at Falls Rocky A (Fig. S1b) and there is a near-complete streamflow record for this site between 1940 and 1986. The average discharge for Watchbed Creek over that time period was

5 $5.64 \times 10^6 \text{ m}^3 \text{ yr}^{-1}$ (Department of Environment, Water, Land and Planning, 2016). For the average annual rainfall of 1.25 m yr^{-1} (Bureau of Meteorology, 2016), the runoff coefficient (i.e., the volume of rainfall that is exported by the stream) was 78%. This is much higher than the runoff coefficients in the eucalypt-dominated catchments of the upper Ovens Valley which range from 6 to 64% (Cartwright and Morgenstern, 2015). That Watchbed Creek exports more rainfall than streams from the eucalypt

10 forests is also apparent in the flow duration curves (Fig. 2b). Relative discharges from Watchbed Creek are around an order of magnitude higher than those from Simmons Creek in the upper Ovens catchment. Simmons Creek has a slightly larger catchment area (6 km^2 vs. 3.5 km^2) and receives similar rainfall but drains eucalypt forest.

3.2 Stable isotope ratios

15 Stable isotope ratios are presented in Table 1 and Fig. 3. Rainfall has $\delta^{18}\text{O}$ values of -7.9 to $-6.5\text{\textperthousand}$ and $\delta^2\text{H}$ values of -40 to $-34\text{\textperthousand}$. The $\delta^{18}\text{O}$ and $\delta^2\text{H}$ values of the peatland water range from -8.3 and $-5.0\text{\textperthousand}$ and -43 to $-26\text{\textperthousand}$, respectively. The eucalyptus forest streams have smaller ranges of $\delta^{18}\text{O}$ and $\delta^2\text{H}$ values (-7.4 to $-5.7\text{\textperthousand}$ and -38 to $-29\text{\textperthousand}$, respectively). As is commonly the case in southeast Australia (Cartwright et al., 2012; Leaney and Herczeg, 1999), the $\delta^{18}\text{O}$ and $\delta^2\text{H}$ values of all waters including rainfall lie to the left of the global and Melbourne meteoric water lines. Overall the waters define an array with a slope of ~ 5 and have D-excess values between 14 and $24\text{\textperthousand}$ with a median of $19\text{\textperthousand}$. These D-excess values are significantly higher than the mean D-excess of the Melbourne meteoric water line of $9.6\text{\textperthousand}$ (Hughes and Crawford, 2012).

20

3.3 Tritium activities

25 The ${}^3\text{H}$ activities of three multi-month rainfall samples from Mount Buffalo are 2.85 TU (12 month sample collected in February 2015), 2.88 TU (9 month sample collected in November 2015), and 2.99 (17 month sample collected in December 2013) (Table 1). Three samples of rainfall collected over

periods of 2 weeks to 3 months in 2014 also from Mount Buffalo have ${}^3\text{H}$ activities of 2.52 to 2.90 TU (Table 1). The sample with the lowest ${}^3\text{H}$ activity represents mainly snow and low-temperature rainfall collected over a 2 week period in July 2014. The ${}^3\text{H}$ activities are within the expected range of ${}^3\text{H}$ activities in rainfall for this region of 2.8 to 3.2 TU (Tadros et al., 2014). Aside from the July 2014 rainfall

5 sample that represents the two weeks of winter precipitation, there is an inverse correlation ($R^2 = 0.69$) between the ${}^3\text{H}$ activities and $\delta^{2\text{H}}$ of rainfall (Fig. 4). Since the rainfall with the higher $\delta^{2\text{H}}$ values has lower D-excess values, there is also a correlation between D-excess and ${}^3\text{H}$ activities. Rainfall from elsewhere in southeast Australia defines broadly similar trends in $\delta^{18\text{O}}$ vs. $\delta^{2\text{H}}$ values and $\delta^{2\text{H}}$ vs ${}^3\text{H}$ values (Table 1, Figs 3, 4).

10 The peatland waters have ${}^3\text{H}$ activities that vary from 2.70 to 3.32 TU (median = 2.75 TU) at Mount Buffalo, 2.90 to 3.17 (median = 3.04 TU) at Falls Creek, and 2.47 to 3.36 (median = 2.77 TU) at Dargo (Table 1, Figs 4, 5). The median ${}^3\text{H}$ activity of the peatland waters as a whole is 2.88 TU. The ${}^3\text{H}$ activities of the peatland water from the three sites are closely similar. Additionally, there are no significant differences in ${}^3\text{H}$ activities of water collected from within the peat and that collected from the streams
15 draining the peat. The ${}^3\text{H}$ activities of waters collected in February 2015 and those collected in November 2015 also overlap. The ${}^3\text{H}$ activities of the peatland waters are locally higher than those of the rainfall samples and several of those waters also have lower $\delta^{2\text{H}}$ values and higher D-excesses than the rainfall (Figs 3, 4).

The eucalyptus forest streams have ${}^3\text{H}$ activities of between 1.56 and 2.35 TU (median = 2.10 TU)
20 (Table 1; Figs 4, 5) that are lower than those of the peatland waters. The ${}^3\text{H}$ activities of the eucalyptus streams overlap with those of river water from the streams in the upper Ovens catchment at low flow conditions in December 2013 and February 2014, which range from 1.63 to 2.28 TU (median = 2.09 TU) (Cartwright and Morgenstern, 2015; Fig. 5).

3.4 Major ion geochemistry

25 Cl concentrations of the peatland waters are between 0.5 and 1.1 mg l⁻¹, which are similar to those of rainfall from Mount Buffalo (0.8 to 1.1 mg l⁻¹) (Fig. 5a, Table 1). Peatland water from Falls Creek has lower Cl concentrations (0.5 to 0.9 mg l⁻¹) than that from the other areas; however, there is no

significant difference between the Cl concentrations of the water extracted from within the peat and that draining the peatlands. Na concentrations of the peatland water range from 0.8 to 2.1 mg l⁻¹, which are higher than those of rainfall (0.6 to 1.0 mg l⁻¹) (Fig. 5b). The eucalypt forest streams have higher Cl (1.1 to 2.6 mg l⁻¹) and Na (3.2 to 5.7 mg l⁻¹) concentrations than any of the peatland water 5 (Figs. 5a, 5b). Molar Na/Cl ratios range from 1.7 to 3.5 in the peatland water and 3.9 to 6.8 in the eucalypt forest streams (Fig. 5d). These Na/Cl ratios are higher than those of Buffalo rainfall, which has Na/Cl ratios of 1.0 to 1.1 that are similar to those generally recorded in southeast Australia (Blackburn and McLeod, 1983; Crosbie et al., 2012).

Molar Cl/Br ratios vary between 340 and 650 in the peatland water and between 550 and 780 in the 10 eucalypt forest streams (Fig. 5c). These ratios are similar to those of Buffalo rainfall (570 to 650) and also similar to the ocean Cl/Br ratio of ~650 (Davis et al., 1998). Other cation/Cl ratios are also higher in the eucalypt forest streams compared with the peatland water, and the water from both these 15 sources has higher cation/Cl ratios than rainfall. Si concentrations in Buffalo rainfall are <0.1 mg l⁻¹ (Fig. 5e) and molar Si/Cl ratios are ~0.1 (Fig. 5f). By contrast, Si concentrations and Si/Cl ratios in the peatland water and eucalypt forest streams are significantly higher (up to 9.8 mg l⁻¹ and 9.5, respectively: Figs 5e, 5f).

There are broad inverse correlations between ³H activities and Na, Cl, and Si concentrations and Na/Cl 20 and Si/Cl ratios (Fig. 5). In general the differences in geochemistry between the peatland water and eucalypt forest streams are more marked than the geochemical variations within those groups. For example, the Si vs. ³H trend for the combined peatland water and eucalypt forest streams has a R² of 0.63, whereas R² values for Si vs. ³H in the peatland water and the eucalyptus forest streams are 0.05 25 and 0.32, respectively. The correlations between major element concentrations and ³H activities are stronger in the eucalypt forest streams (R² values of 0.32 to 0.87) than in the peatland waters (R² values of 0.05 to 0.24). The trends in ³H activities vs. major ion concentrations or ratios in the eucalyptus forest streams from the Victorian Alps are similar to those of the upper Ovens catchment as a whole.

4. Discussion

This section combines the major ion geochemistry, stable isotope data, and ${}^3\text{H}$ activities to determine the mean transit times of the waters from the peatlands and eucalyptus forest streams and assesses the major geochemical processes that impact these waters.

5 4.1 Modern rainfall ${}^3\text{H}$ activities

Understanding the ${}^3\text{H}$ activities of the water that recharges the catchments is critically important in estimating mean transit times. The three longer-term (9 to 17 month) rainfall samples have ${}^3\text{H}$ activities of between 2.85 and 2.99 TU, which lie within the predicted ${}^3\text{H}$ activity of rainfall in this area of 2.8 to 3.2 TU (Tadros et al., 2014). However, the observation that the peatland water has ${}^3\text{H}$ activities that are locally up to 3.35 TU indicates that it is not possible to use the rainfall ${}^3\text{H}$ activities 10 as the ${}^3\text{H}$ activity of recharge for all of the peatland waters.

There may be spatial variations in rainfall ${}^3\text{H}$ activities, especially between the three areas. The observation, however, that peatland water at Mount Buffalo from <5 km from the rainfall gauge has a ${}^3\text{H}$ activity of up to 3.32 TU suggests that this cannot be the only explanation. The higher ${}^3\text{H}$ activities 15 in the peatland waters potentially reflect preferential recharge by spring rainfall. Maximum ${}^3\text{H}$ activities in Australian rainfall are recorded in early spring (August to September) as this is the time of maximum transport of water vapour with high ${}^3\text{H}$ activities from the stratosphere to the troposphere (Tadros et al., 2014). Stratospheric moisture also has lower $\delta^2\text{H}$ values and higher D-excesses than tropospheric moisture (Bony et al., 2008). Thus the variation in the relative ratios of stratospheric to 20 tropospheric moisture would also explain the observations that rainfall samples with higher ${}^3\text{H}$ activities have lower $\delta^2\text{H}$ values (Fig. 4) and higher D-excess values (Fig. 3).

Some peatland waters have lower $\delta^2\text{H}$ values than those of the rainfall. These potentially record recharge by rainfall that has a high proportion of low $\delta^2\text{H}$ stratospheric moisture. Such rainfall would also be expected to have higher ${}^3\text{H}$ activities than average rainfall. While it is difficult to precisely 25 constrain the ${}^3\text{H}$ of seasonal recharge, extending the rainfall $\delta^2\text{H}$ vs. ${}^3\text{H}$ trend defined by the Mount Buffalo rainfall samples in Fig. 4 to the lowest $\delta^2\text{H}$ value of the peatland waters ($-43\text{\textperthousand}$) yields a ${}^3\text{H}$ activity of ~ 3.4 TU, which is similar to the highest ${}^3\text{H}$ activities recorded in the peatland waters. This is

~14% higher than the ${}^3\text{H}$ activities of the rainfall samples, which is well within the seasonal variation of ${}^3\text{H}$ activities of Australian rainfall (Tadros et al., 2014).

That some of the peatland waters with high ${}^3\text{H}$ activities have higher $\delta^2\text{H}$ values is likely due to subsequent evaporation (Fig. 4). As discussed below, the major ion geochemistry also implies that 5 evaporation has affected these waters. Evaporation at a humidity of 50 to 70%, which is characteristic of these Alpine areas in summer (Bureau of Meteorology, 2016), produces arrays of $\delta^{18}\text{O}$ and $\delta^2\text{H}$ values with slopes of 4 to 5 (Clark and Fritz, 1999). Thus the $\delta^{18}\text{O}$ and $\delta^2\text{H}$ values of the waters (Fig. 3) probably reflects both initial variations in stable isotope ratios and subsequent evaporation. Assuming 10 that the mass-dependant isotope fractionation of ${}^3\text{H}/{}^1\text{H}$ is approximately double that of ${}^2\text{H}/{}^1\text{H}$, a 10‰ increase in $\delta^2\text{H}$ values would equate to a ~2% increase in ${}^3\text{H}$ activities, which is approximately the analytical precision.

4.2 Mean transit times

Mean transit times (Table 2, Fig. 6a) were initially calculated using an exponential-piston flow model with an EPM ratio of 0.33 via Eqs (1 and 2). The soils and shallow aquifers are unconfined and likely to 15 exhibit exponential flow below the water table; however, recharge through the unsaturated zone will most likely resemble piston flow. A similar flow model successfully reproduces time-series of ${}^3\text{H}$ activities in upland catchments in New Zealand (Morgenstern et al., 2010). Given that the waters were sampled at baseflow conditions during the late spring or summer, which represent the driest months, it was assumed that there was a single store of water present rather than a mixture of recent rainfall 20 and older water. While the exponential-piston flow model plausibly represents the flow systems, it is not possible to independently test its veracity. Hence, mean transit times were also calculated using the exponential flow model with a higher proportion of piston flow (EPM ratio of 1), the exponential flow model, and the dispersion model with $D_p = 0.1$ and 1.0 which are appropriate values for flow systems of this scale (Maloszewski, 2000) (Table 2, Fig. 6a).

25 The annual average ${}^3\text{H}$ activities of rainfall in Melbourne, which is ~200 km to the southwest, from the International Atomic Energy Agency Global Network of Isotopes in Precipitation program as summarised by Tadros et al. (2014) were used as the ${}^3\text{H}$ input. Rainfall ${}^3\text{H}$ activities reached ~62 TU in

1965 and then declined exponentially to present-day values (Tadros et al., 2014). The calculations initially adopted a present-day ${}^3\text{H}$ activity of recharge of 3.4 TU (as discussed above). A ${}^3\text{H}$ activity of 3.4 TU was also used for recharge from prior to the atmospheric nuclear tests.

Mean transit times from the exponential piston flow model with an EPM ratio of 0.33 are up to 6.4 years with a median of 3.0 years (Table 2). For the range of ${}^3\text{H}$ activities in these peatland waters, between the mean transit times estimated from the different lumped parameter models are similar (Table 2, Fig. 6a). The exponential-piston flow model with an EPM ratio of 1 yields mean transit times of up to 6.0 years with a median of 2.9 years. The exponential flow model produces mean transit times of up to 7.4 years with a median of 3.1 years. The dispersion model yields mean transit times of up to 10 6.0 years with a median of 2.8 years ($D_p = 0.1$) and 8.0 years with a median of 3.5 years ($D_p = 1.0$).

For a water with a ${}^3\text{H}$ activity of 3 TU, propagating the analytical uncertainty of $\pm 2\%$ produces an uncertainty in mean transit times of ± 0.3 years. Uncertainties in calculated mean transit times for the high ${}^3\text{H}$ samples mainly arise from the assumed ${}^3\text{H}$ activity of the recharging water (Fig. 6b), which as discussed above is difficult to constrain precisely. This will be illustrated for the exponential-piston flow model with an EPM ratio of 0.33, but similar variations would be observed for the other models. Utilising a ${}^3\text{H}$ activity of 3.0 TU for modern and pre-bomb pulse rainfall based on the ${}^3\text{H}$ activities of the rainfall samples (Table 1), yields mean transit times of up to 4.0 years with a median of <1 year (Table 2). However, in this case a large number of peatland waters have ${}^3\text{H}$ activities that are higher than the rainfall activities and for those waters, a ${}^3\text{H}$ activity of 3.0 TU for the recharging water is not 15 realistic. Adopting a ${}^3\text{H}$ activity of 3.2 TU, which is the upper limit of the estimate for annual rainfall in this area (Tadros et al., 2004) yields mean transit times of up to 5.4 years with a median of 1.8 years. In this case two peatland waters (Dargo D and Buffalo Cresta A) have ${}^3\text{H}$ activities that are higher than 20 the assumed recharge ${}^3\text{H}$ activities. Given the likelihood that seasonal recharge has occurred and thus the ${}^3\text{H}$ activity of the recharging water may be locally variable, it is unrealistic to differentiate mean 25 transit times of <1 year.

By contrast with the peatland waters, the eucalypt forest streams have much longer mean transit times that are relatively insensitive to the assumed ${}^3\text{H}$ activity of recharge (Fig. 6b). For the

exponential-piston flow model with an EPM ratio of 0.33 and a modern and pre-bomb pulse rainfall activity of 3.0 TU (which assumes recharge has the ${}^3\text{H}$ activity of average rainfall), mean transit times range from 5.3 to 28.6 years with a median of 9.5 years (Table 2). Adopting a ${}^3\text{H}$ activity for recharge of 3.2 TU, the mean transit times range from 6.9 to 28.8 years with a median of 10.8 years and if the 5 ${}^3\text{H}$ activity of recharge was 3.4 TU, the mean transit times are 7.8 to 28.9 years with a median of 11.5 years. These mean transit times are within the range of those of the much larger (6 to 1240 km²) catchments in the upper Ovens Valley that are also dominated by eucalypt forest. Mean transit times of river water in December 2013 and February 2014 in the upper Ovens Valley calculated using the same exponential-piston flow model and a ${}^3\text{H}$ activity of recharge of 3.0 TU are 7 to 30 years 10 (Cartwright and Morgenstern, 2015).

For the eucalypt forest streams there are larger uncertainties in mean transit times produced by the different lumped parameter models (Table 2, Fig. 6a). The range in mean transit times for a water with a ${}^3\text{H}$ activity of 2 TU calculated from the exponential flow model, the exponential-piston flow model with EPM ratios of 0.33 and 1, and the dispersion model with $D_p = 0.1$ and $D_p = 1$ is ~ 4.5 years. For a 15 water with a ${}^3\text{H}$ activity of 1.5 TU the range in mean transit times from those models is ~ 13 years. Uncertainties as to the most appropriate lumped parameter model thus represent a significant source of uncertainty in these calculations. However, overall the water in these streams has mean transit times of years to decades and is significantly older than that from the peatlands. Propagating the analytical uncertainty in ${}^3\text{H}$ activities (Table 2) also results in uncertainties in mean transit times of 20 ± 0.5 years for a water with a ${}^3\text{H}$ activity of 2 TU.

Aggregation of water with different mean transit times also introduces uncertainty in the calculated mean transit times (Kirchner, 2016a; Stewart et al., 2016). Figure 8 illustrates the impact of mixing different proportions of water with mean transit times of between 10 and 50 years (appropriate for the eucalypt forest waters) on the calculated mean transit times. The actual mean transit time 25 represents the mean transit time that calculated from the weighted average of the transit times of the mixed waters. The apparent mean transit time is calculated from the ${}^3\text{H}$ activity of the mixed water again using the exponential piston flow model with an EPM ratio of 0.33. The apparent mean transit times are less than the actual mean transit times with the greatest difference ($\sim 13\%$) occurring when

there are approximately equal proportions of two end members with mean transit times of 10 and 50 years. The difference between actual and apparent mean transit times decreases when multiple end-members are aggregated (shaded field). For example the apparent mean transit time calculated from an equal mixture of nine waters with transit times of 10, 15, 20, 25, 30, 35, 40, 45, and 50 years is 28.9

5 years, which is within 4% of the actual mean transit time of 30 years. The relative difference between apparent and actual mean transit times are similar when other lumped parameter models are used. Mixing waters with a range of mean transit times between 1 and 5 years (which would be appropriate for the peatland waters) produces similar relative differences. Thus aggregation introduces uncertainties that are of similar order of magnitude to those resulting from other uncertainties in the

10 calculations (discussed above).

There are uncertainties in the calculated mean transit times resulting from uncertainties in the ^{3}H activity of recharge, the most appropriate lumped parameter model, and aggregation. However, the conclusion that the mean transit times of water in the eucalypt forest catchments range from several years to decades and are significantly longer than those in the peatlands remains robust. Mean transit

15 times of the peatland waters are unlikely to be more than a few years and may be mainly less than 2 years depending on the ^{3}H activity of recharge. As noted above, the ^{3}H activities of the water from the piezometers in the peatlands are similar to the water that drains the peat. The water that drains the peat is likely derived mainly from the acrotelm (Western et al., 2009; Grover and Baldock, 2013), presuming that the piezometers which were inserted into the lower levels of the peat sampled water

20 from the catotelm, this observation implies that the catotelm is not a store of older water.

4.3 Major ion tracers

The major ion geochemistry allows the main geochemical processes to be understood and also can provide first-order estimates of mean transit times. Overall, the observation that the Cl/Br ratios in the peatland water and the eucalypt forest streams have molar Cl/Br ratios that cluster around those

25 of the rainfall implies that, in common with the majority of groundwater and surface water in southeast Australia, the vast majority of Cl is derived from the rainfall and concentrated by evapotranspiration (Cartwright et al., 2006; Herczeg et al., 2001). Other potential sources of Cl (such

as dissolution of halite in the unsaturated zone) produce water with high Cl/Br ratios and can thus be discounted.

The higher Cl concentrations in the eucalypt forest streams compared with that from the peatland water reflects higher net evapotranspiration rates in the eucalypt forest catchments. Some of the

5 increase in the concentration of the other major ions such as Na in the eucalypt forest streams and peatland water over those in rainfall will also be due to evapotranspiration. The adsorption of Br by organic matter (Gerritse and George, 1988) may locally increase Cl/Br ratios if the pool of organic matter is increasing. By contrast, a net degradation of organic matter releases Br producing lower Cl/Br ratios. The wider range of Cl/Br ratios in the peatland water may reflect that, locally, the volume 10 of organic matter is increasing whereas elsewhere it is degrading. The far more homogeneous Cl/Br ratios in the eucalypt forest streams indicate that either the organic matter content of those catchments is relatively stable or that the waters are better mixed and any local variations in Cl/Br ratios have been homogenised. This homogenisation is consistent with longer mean transit times in the eucalypt forest streams.

15 The increase in cation/Cl and Si/Cl ratios in the peatland and eucalypt forest waters over those in rainfall is interpreted to be due to silicate weathering (c.f., Herczeg and Edmunds, 2000). As rainfall contains $<0.1 \text{ mg l}^{-1}$ Si, evapotranspiration will not increase Si concentrations appreciable and the vast majority of the Si will be derived from silicate weathering. The eucalypt forest streams have higher cation/Cl and Si/Cl ratios compared with the peatland water and thus records higher degrees of 20 weathering. This is likely due to two factors. Firstly, the eucalypt forest catchments are developed on weathered regolith and the flow of water through the regolith will promote mineral dissolution. Common minerals in the regolith include plagioclase and alkali feldspars (Cartwright and Morgenstern, 2012) and the dissolution of these will provide Si, Na, Ca, and K. By contrast, the peatlands are developed on less weathered rocks, which limits the potential for mineral dissolution; although there 25 clearly has been sufficient weathering to produce the elevated cation/Cl and Si/Cl ratios. There is commonly a thin (<20 cm thick) layer of regolith at the base of the peat and fragments of basement rock within the lower layers of the peat that are likely being weathered by the peatland water.

Secondly, the longer mean transit times in the eucalypt forest catchments allow the silicate weathering reactions to progress further than in the peatlands.

4.4 Controls on mean transit times

As with the Ovens catchment as a whole, there is no correlation between ${}^3\text{H}$ activities and catchment

5 areas either within or between the eucalypt forest and peatland catchments (Fig. 7). Elsewhere, inverse correlations between catchment slope and mean transit times have been documented (McGuire et al., 2005). Catchment slopes have not been calculated in this study (and would be difficult do so in the peatlands given the limitations of the DEM). However, the observation that the eucalypt forests occur in gullies that invariably have steeper slopes than the peatlands but contain water with 10 longer mean transit times indicates that, in this case, catchment slopes cannot explain the difference in mean transit times between the two catchment types.

The difference in the mean transit times between the peatland water and the eucalypt forest streams

is likely the combination of two factors. Firstly the high evapotranspiration rates of the eucalypt forests (Allison et al., 1990) results in low recharge rates that in turn increase the transit times.

15 Secondly, differences in the depth of weathering in the catchments and the development of deeper flow paths is also likely to be important. Most of the peatlands are developed on relatively unweathered basement rocks and the majority of the water is stored within the peat itself (Grover and Baldock, 2013; Western et al., 2009). Given that most of the peat is <2 m thick, this results in a shallow reservoir of water underlain by bedrock with very low hydraulic conductivities. By contrast, 20 groundwater in the eucalypt gullies is partially hosted in weathered regolith that is locally several metres thick. The gullies may be developed where weathering is greater due to the presence of joints and/or faults that will also host groundwater flow (Shugg, 1987). The presence of weathered and fractured bedrock on steep slopes conceivably allows long groundwater flow paths to develop that will increase transit times.

25 The correlation between major ion concentrations and ${}^3\text{H}$ activities may allow a first-order estimate of relative mean transit times to be made, which is useful in extending studies such as this to adjacent catchments. Caution must be exercised, however, in using the datasets as a whole as the geochemistry

may partially reflect differences in the characteristics of the peatland and eucalypt forest catchments (specifically whether the water flows through the regolith or is contained within the peat) rather than solely the mean transit times. Nevertheless, in the catchments studied here there are broad correlations between ${}^3\text{H}$ activities and major ion concentrations within both the peatland water and

5 the eucalypt forest streams, which would permit estimations of relative mean transit times.

Streamflow (Q) is related to the mean transit time (MTT) and the volume of water held in storage (V) via $Q = V / \text{MTT}$ (Maloszewski and Zuber, 1982). This relationship is commonly used to estimate V where MTT has been calculated and Q measured (e.g., Morgenstern et al., 2010). However, in ungauged peatland catchments such as these it is possible to estimate Q if the volume of peat can be

10 estimated and MTT is known. The area drained by the stream at Falls Rocky A is $3.5 \times 10^6 \text{ m}^2$ and for a peat thickness of 0.5 to 1 m (which is consistent with observations at this site), $V = 1.75 \text{ to } 3.5 \times 10^6 \text{ m}^3$. Adopting a range of mean transit times of 0.5 to 2.5 years (Table 2) yields estimates of Q of 7.0×10^5 to $7.0 \times 10^6 \text{ m}^3 \text{ yr}^{-1}$, which span the measured average discharge of $5.64 \times 10^6 \text{ m}^3 \text{ yr}^{-1}$. Presuming that the parameterisation is appropriate, the correspondence between calculated and observed streamflows

15 occurs when mean transit times are < 1 year, which suggests that the ${}^3\text{H}$ activities of rainfall which recharges the peat are not significantly higher than those discussed above. Carrying out these calculations on the Victorian peatland water is difficult as Q tends to ∞ as the MTT approaches 0. In ungauged peatland catchments where mean transit times are longer, however, this would be a viable method of estimating Q .

20 **5. Conclusions**

The mean transit times in peatland water in southeast Australia are less than 6.5 years and in many cases substantially shorter. The short mean transit times implies that the peat is susceptible to drying if there are successive years of below average rainfall. In turn this makes the peat vulnerable to damage during the periodic bushfires that also occur during the summers in drought periods. The

25 majority of southeast Australia underwent a major drought (the “millennium drought”) between 1995 and 2010 (Bureau of Meteorology, 2016) during which time there were major bushfires in the

Australian Alps, especially in 2003 and 2009. Although mainly affecting the eucalypt forests, locally these bushfires also impacted the peatlands (Arthur Rylah Institute, 2016).

The observation that the water from within the peat yields similar mean transit times to that draining the peat implies that there is not likely to be older water stored within the deeper layers. This may be

5 because the peat in the Victorian Alps is shallow and consequently stores little water. The peatlands do not act as a long-lived store of water to the river systems. Given their small total area, there would be little impact of peatland drying to the hydrology of the lower reaches of the adjacent catchments.

However, drying of the peat could impact the hydrology of the small upland streams that form an integral part of the landscape and ecosystems of the alpine areas. The observation that even in small

10 eucalypt forest catchments the stream water has mean transit times of several years to decades indicates that they are likely to be more resilient to short-term variations in rainfall. As a whole, the river catchments in the Victorian Alps are eucalypt dominated, which implies that the river systems are likely to be sustained by baseflow even during prolonged drought periods, and indeed many of these streams continued to flow through the millennium drought.

15 More generally this study illustrates that the combination of ${}^3\text{H}$ and major ion geochemistry allows both the timescales of water movement and the hydrogeochemical processes in these catchments to be understood. As noted by Western et al. (2009), there is a common perception that, due to their high water contents and organic rich soils, peatlands represent long-term water stores and indeed this was the premise that this study set out to test. However, this is not the case in this study and possibly 20 not elsewhere. For example, the upland catchments in the United Kingdom that include extensive peat areas have transit times are <5 years (Kirchner et al., 2012; Soulsby et al., 2006; Hrachowitz et al., 2013; Benettin et al., 2015) and the Zhurucay area in Ecuador where mean transit times are <1 year (Mosquera et al., 2016).

25 The study has determined transit times using individual ${}^3\text{H}$ measurements, which is possible in the southern hemisphere due to the decline of the bomb-pulse ${}^3\text{H}$. While this removes the requirement of collecting data over several years and does not require the assumption of steady-state flow systems, it is not possible to test the appropriateness of the lumped parameter models. Differences between

the mean transit times estimated from the different lumped parameter models is one of the main uncertainties, especially where the mean transit times are in excess of a few years. Uncertainties in the ${}^3\text{H}$ activities of recharge and errors caused by aggregation of water with different mean transit times also impact these calculations (as they do the calculations based on time-series data).

5 Irrespective of these uncertainties, the fact that the relative difference in mean transit times between waters is readily calculated is valuable in understanding catchments.

6. Data Availability

All geochemical data used in this study are contained in Table 1. Streamflow data are publicly available from the Victorian State Government Department of Environment, Land, Water and Planning

10 (<http://data.water.vic.gov.au/monitoring.htm>).

Author contributions. U. Morgenstern was responsible for the ${}^3\text{H}$ analyses. I. Cartwright undertook the sampling program and oversaw the analysis of the other geochemical parameters. I. Cartwright and U. Morgenstern prepared the manuscript.

15

Acknowledgements. Funding for this project was provided by Monash University and the National Centre for Groundwater Research and Training. The National Centre for Groundwater Research and Training is an Australian Government initiative supported by the Australian Research Council and the National Water Commission via Special Research Initiative SR0800001. Massimo Raveggi and Rachael

20 Pearson carried out the geochemical analyses at Monash University. E Timbe, Markus Hrachowitz, and an anonymous reviewer, are thanked for their helpful and perceptive comments that improved the paper.

References

Allison, G. B., Cook, P. G., Barnett, S. R., Walker, G. R., Jolly, I. D., and Hughes, M. W.: Land clearance
25 and river salinisation in the western Murray Basin, Australia, *Journal of Hydrology*, 119, 1-20, 1990.

Arthur Rylah Institute.: Fire Ecology and Recovery, available at

<http://www.depi.vic.gov.au/environment-and-wildlife/arthur-rylah-institute/research-themes/fire-ecology-and-recovery>, last accessed July 2016.

Benettin, P., Kirchner, J. W., Rinaldo, A., and Botter, G.: Modeling chloride transport using travel time

5 distributions at Plynlimon, Wales, *Water Resources Research*, 51, 3259-3276, 2015.

Blackburn, G. and McLeod, S.: Salinity of atmospheric precipitation in the Murray Darling Drainage Division, Australia, *Australian Journal of Soil Research*, 21, 400-434, 1983.

Bony, S., Risi, C., and Vimeux, F.: Influence of convective processes on the isotopic composition ($\delta^{18}\text{O}$ and δD) of precipitation and water vapor in the tropics: 1. Radiative-convective equilibrium and

10 Tropical Ocean–Global Atmosphere–Coupled Ocean-Atmosphere Response Experiment (TOGA-COARE) simulations, *Journal of Geophysical Research*, 113, D19305, doi:10.1029/12008JD009942, 2008.

Bureau of Meteorology: Commonwealth of Australia Bureau of Meteorology, available at:

<http://www.bom.gov.au>, last access: July 2016.

15 Cartwright, I. and Morgenstern, U.: Constraining groundwater recharge and the rate of geochemical processes using tritium and major ion geochemistry: Ovens catchment, southeast Australia, *Journal of Hydrology*, 475, 137-149, 2012.

Cartwright, I. and Morgenstern, U.: Transit times from rainfall to baseflow in headwater catchments estimated using tritium: the Ovens River, Australia, *Hydrology and Earth System Sciences*, 19, 3771-

20 3785, 2015.

Cartwright, I., Weaver, T. R., Cendón, D. I., Fifield, L. K., Tweed, S. O., Petrides, B., and Swane, I.: Constraining groundwater flow, residence times, inter-aquifer mixing, and aquifer properties using environmental isotopes in the southeast Murray Basin, Australia, *Applied Geochemistry*, 27, 1698-1709, 2012.

Cartwright, I., Weaver, T. R., and Fifield, L. K.: Cl/Br ratios and environmental isotopes as indicators of recharge variability and groundwater flow: An example from the southeast Murray Basin, Australia, Chemical Geology, 231, 38-56, 2006.

Charman, D. J., Aravena, R., Bryant, C. L., and Harkness, D. D.: Carbon isotopes in peat, DOC, CO₂, and CH₄ in a Holocene peatland on Dartmoor, Southwest England, Geology, 27, 539-542, 1999.

Clark, I. D. and Fritz, P.: Environmental Isotopes in Hydrogeology, Lewis, New York, USA, 1997.

Cook, P. G. and Bohlke, J. K.: Determining timescales for groundwater flow and solute transport. In: Environmental Tracers in Subsurface Hydrology, Cook, P. G. and Herczeg, A. L. (Eds.), Kluwer, Boston, USA, 1-30, 2000.

10 Coplen, T. B.: Normalization of oxygen and hydrogen isotope data, Chemical Geology, 72, 293-297, 1988.

Costin, A. B.: Carbon-14 dates from the Snowy Mountains area, southeastern Australia, and their interpretation, Quaternary Research, 2, 579-590, 1972.

Crosbie, R., Morrow, D., Cresswell, R., Leaney, F., Lamontagne, S., and Lefournour, M.: New insights 15 to the chemical and isotopic composition of rainfall across Australia, CSIRO Water for a Healthy Country Flagship, Australia., 2012

Davis, S. N., Whittemore, D. O., and Fabryka-Martin, J.: Uses of chloride/bromide ratios in studies of potable water, Ground Water, 36, 338-351, 1998.

Department of Environment, Land, Water and Planning: State Government Victoria Department of 20 Environment Environment, Land, Water and Planning Water Measurement Information System, available at: <http://data.water.vic.gov.au/monitoring.htm>, last access: July 2016.

Dever, L., Hillaire-Marcel, C., and Fontes, J. C.: Isotopic composition, geochemistry and genesis of ice lenses (palsen) in peat bogs; New Quebec, Canada, Journal of Hydrology, 71, 107-130, 1984.

Dixon, R. K., Brown, S., Houghton, R. A., Solomon, A. M., Trexler, M. C., and Wisniewski, J.: Carbon 25 pools and flux of global forest ecosystems, Science, 263, 185-190, 1994.

Energy and Earth Resources: State Government Victoria Department of Economic Development, Jobs, Transport and Resources, available at: <http://www.energyandresources.vic.gov.au/earth-resources/maps-reports-and-data/geovic>, last access: July 2016.

Gerritse, R. G. and George, R. J.: The role of soil organic matter in the geochemical cycling of chloride

5 and bromide, *Journal of Hydrology*, 101, 83-85, 1988.

Gorham, E.: Northern peatlands: role in the carbon cycle and probable responses to climatic warming, *Ecological Applications*, 1, 182-195, 1991.

Grover, S. P. P. and Baldock, J. A.: Carbon decomposition processes in a peat from the Australian Alps, *European Journal of Soil Science*, 61, 217-230, 2010.

10 Grover, S. P. P. and Baldock, J. A.: The link between peat hydrology and decomposition: Beyond von Post, *Journal of Hydrology*, 479, 130-138, 2013.

Grover, S. P. P., McKenzie, B. M., Baldock, J. A., and Papst, W. A.: Chemical characterisation of bog peat and dried peat of the Australian Alps, *Australian Journal of Soil Research*, 43, 963-971, 2005.

15 Herczeg, A. L., Dogramaci, S. S., and Leaney, F. W.: Origin of dissolved salts in a large, semi-arid groundwater system: Murray Basin, Australia, *Marine and Freshwater Resources*, 52, 41-52, 2001.

Herczeg, A. L. and Edmunds, W. M.: Inorganic ions as tracers. In: *Environmental Tracers in Subsurface Hydrology*, Cook, P. and Herczeg, A. (Eds.), Kluwer Academic Publishers, Boston, 31-77, 2000.

20 Hrachowitz, M., Savenije, H., Bogaard, T. A., Tetzlaff, D., and Soulsby, C.: What can flux tracking teach us about water age distribution patterns and their temporal dynamics?, *Hydrology and Earth System Sciences*, 17, 533-564, 2013

Hrachowitz, M., Soulsby, C., Tetzlaff, D., and Speed, M.: Catchment transit times and landscape controls - Does scale matter?, *Hydrological Processes*, 24, 117-125, 2010.

25 Hughes, C. E. and Crawford, J.: A new precipitation weighted method for determining the meteoric water line for hydrological applications demonstrated using Australian and global GNIP data, *Journal of Hydrology*, 464-465, 344-351, 2012.

International Atomic Energy Association: Global Network of Isotopes in Precipitation, available at:

<http://www.iaea.org/water>, last access: July 2016.

Jurgens, B. C., Bohlke, J. K., and Eberts, S. M.: TracerLPM (Version 1): An Excel® workbook for interpreting groundwater age distributions from environmental tracer data, U.S. Geological Survey

5 Techniques and Methods Report 4-F3, 2012.

Kirchner, J. W.: Aggregation in environmental systems – Part 1: Seasonal tracer cycles quantify young water fractions, but not mean transit times, in spatially heterogeneous catchments, *Hydrology and Earth System Sciences*, 20, 279-297, 2016a.

Kirchner, J. W.: Aggregation in environmental systems – Part 2: Catchment mean transit times and

10 young water fractions under hydrologic nonstationarity, *Hydrology and Earth System Sciences*, 20, 299-328, 2016b.

Kirchner, J. W., Tetzlaff, D., and Soulsby, C.: Comparing chloride and water isotopes as hydrological tracers in two Scottish catchments, *Hydrological Processes*, 24, 1631-1645, 2010.

Leaney, F. and Herczeg, A.: The origin of fresh groundwater in the SW Murray Basin and its potential 15 for salinisation, CSIRO Land and Water Technical Report 7/99, Adelaide, 1999.

Maloszewski, P.: Lumped-parameter models as a tool for determining the hydrological parameters of some groundwater systems based on isotope data, IAHS-AISH Publication, 2000. 271-276, 2000.

Maloszewski, P. and Zuber, A.: Determining the turnover time of groundwater systems with the aid of environmental tracers. 1. Models and their applicability, *Journal of Hydrology*, 57, 207-231, 1982.

20 Mažeika, J., Guobute, R., Kibirkštis, G., Petrošius, R., Skuratovič, Ž., and Taminskas, J.: The use of carbon-14 and Tritium for peat and water dynamics characterization: Case of Čepkeliai peatland, southeastern Lithuania, *Geochronometria*, 34, 41-48, 2009.

McDonnell, J. J., McGuire, K., Aggarwal, P., Beven, K. J., Biondi, D., Destouni, G., Dunn, S., James, A., Kirchner, J., Kraft, P., Lyon, S., Maloszewski, P., Newman, B., Pfister, L., Rinaldo, A., Rodhe, A.,

25 Sayama, T., Seibert, J., Solomon, K., Soulsby, C., Stewart, M., Tetzlaff, D., Tobin, C., Troch, P., Weiler, M., Western, A., Wörman, A., and Wrede, S.: How old is streamwater? Open questions in

catchment transit time conceptualization, modelling and analysis, *Hydrological Processes*, 24, 1745-1754, 2010.

McDougall, K. L.: *The Alpine Vegetation of the Bogong High Plains.*, Environmental Studies Publication No. 357, Ministry for Conservation, Melbourne, 1982.

5 McGuire, K. J. and McDonnell, J. J.: A review and evaluation of catchment transit time modeling, *Journal of Hydrology*, 330, 534-546, 2006.

McGuire, K. J., McDonnell, J. J., Weiler, M., Kendall, C., McGlynn, B. L., Welker, J. M., and Seibert, J.: The role of topography on catchment-scale water residence time, *Water Resources Research*, 41, 1-14, 2005.

10 Michel, R.L: Residence times in river basins as determined by analysis of long-term tritium records, *Journal of Hydrology*, 130, 367-378, 1992.

Morgenstern, U. and Daughney, C. J.: Groundwater age for identification of baseline groundwater quality and impacts of land-use intensification - The National Groundwater Monitoring Programme of New Zealand, *Journal of Hydrology*, 456-457, 79-93, 2012.

15 Morgenstern, U., Stewart, M. K., and Stenger, R.: Dating of streamwater using tritium in a post nuclear bomb pulse world: Continuous variation of mean transit time with streamflow, *Hydrology and Earth System Sciences*, 14, 2289-2301, 2010.

Morgenstern, U. and Taylor, C. B.: Ultra low-level tritium measurement using electrolytic enrichment and LSC, *Isotopes in Environmental and Health Studies*, 45, 96-117, 2009.

20 Morris, P. J. and Waddington, J. M.: Groundwater residence time distributions in peatlands: Implications for peat decomposition and accumulation, *Water Resources Research*, 47, W02511, doi:10.1029/2010WR009492, 2011.

Mosquera, G. M., Segura, C., Vaché, K. B., Windhorst, D., Breuer, L., and Crespo, P.: Insights into the water mean transit time in a high-elevation tropical ecosystem, *Hydrology and Earth System Sciences*, 20, 2987-3004

Page, S. E., Siegert, F., Rieley, J. O., Boehm, H. D. V., Jaya, A., and Limin, S.: The amount of carbon released from peat and forest fires in Indonesia during 1997, *Nature*, 420, 61-65, 2002.

Shugg, A.: *Hydrogeology of the Upper Ovens Valley*, Report Victoria Department of Industry, Technology and Resources 5, Melbourne, 1987.

5 Siegel, D. I., Chanton, J. P., Glaser, P. H., Chasar, L. S., and Rosenberry, D. O.: Estimating methane production rates in bogs and landfills by deuterium enrichment of pore water, *Global Biogeochemical Cycles*, 15, 967-975, 2001.

Soulsby, C., Tetzlaff, D., Rodgers, P., Dunn, S., and Waldron, S.: Runoff processes, stream water residence times and controlling landscape characteristics in a mesoscale catchment: An initial 10 evaluation, *Journal of Hydrology*, 325, 197-221, 2006.

Stewart, M. K., Morgenstern, U., and McDonnell, J. J.: Truncation of stream residence time: How the use of stable isotopes has skewed our concept of streamwater age and origin, *Hydrological Processes*, 24, 1646-1659, 2010.

Stewart, M. K., Morgenstern, U., Gusyev, M. A., and Maloszewski, P.: Aggregation effects on tritium-based mean transit times and young water fractions in spatially heterogeneous catchments and 15 groundwater systems, and implications for past and future applications of tritium, *Hydrology and Earth System Sciences Discussion*, doi:10.5194/hess-2016-532, 2016

Tadros, C. V., Hughes, C. E., Crawford, J., Hollins, S. E., and Chisari, R.: Tritium in Australian precipitation: A 50 year record, *Journal of Hydrology*, 513, 262-273, 2014.

20 Tetzlaff, D., Birkel, C., Dick, J., Geris, J., Soulsby, C. imbe, E., Windhorst, D., Celleri, R.: Storage dynamics in hydromedical units control hillslope connectivity, runoff generation, and the evolution of catchment transit time distributions, *Water Resources Research*, 50, 969-985, 2014.

Timbe, L., Crespo, P., Frede, H.-G., Feyen, J., and Breuer, L.: Sampling frequency trade-offs in the 25 assessment of mean transit times of tropical montane catchment waters under semi-steady-state conditions, *Hydrology and Earth Systems Sciences*, 19, 1153-1168, 2025.

van den Berg, A. H. M., Wilman, C. E., Morand, V. J., McHaffie, I. W., Simmons, B. A., Quinn, C., and Westcott, A.: Buffalo 1:100 000 map area geological report 124. GeoScience Victoria, Melbourne, 2004.

Van Der Werf, G. R., Randerson, J. T., Giglio, L., Collatz, G. J., Mu, M., Kasibhatla, P. S., Morton, D. C.,

5 Defries, R. S., Jin, Y., and Van Leeuwen, T. T.: Global fire emissions and the contribution of deforestation, savanna, forest, agricultural, and peat fires (1997-2009), *Atmospheric Chemistry and Physics*, 10, 11707-11735, 2010.

Western, A., Rutherford, I., Sirawardena, L., Lawrence, R., P., G., Coates, F., and White, M.: The Geography and Hydrology of High Country Peatlands in Victoria. Part 2: The Influence of Peatlands

10 on Catchment Hydrology, Arthur Rylah Institute for Environmental Research Technical Report No. 174. Department of Sustainability and Environment, Victoria, 2009.

Zuber, A., Witczak, S., Rozanski, K., Sliwka, I., Opoka, M., Mochalski, P., Kuc, T., Karlikowska, J., Kania, J., Jackowicz-Korczynski, M., and Dulinski, M.: Groundwater dating with ^{3}H and SF_6 in relation to mixing patterns, transport modelling and hydrochemistry, *Hydrological Processes*, 19, 2247–2275,

15 2005.

Figure Captions

Fig. 1. Location of study sites in northeast Victoria superimposed on the digital elevation model. Places: Br = Bright; Da = Dargo; MB = Mount Buffalo; MtB = Mount Beauty; MH = Mount Hotham; My = Myrtleford. FFA and FFB are the Falls Forest sampling sites A & B, other sampling sites are in the 5 indicated study areas (see Supplementary Figure S1). Catchment boundaries from Department of Environment, Land, Water and Planning (2016), elevations are relative to the Australian Height Datum (AHD).

Fig. 2a. Streamflow at Watchbed Creek which drains peatlands at Falls Creek (Fig. 1) between 1984 and 1987. **2b.** Flow duration curves for Watchbed Creek and Simmons Creek, which drains eucalyptus 10 forest in the Upper Ovens (Fig. 1). Data from Department of Environment, Land, Water and Planning (2016).

Fig. 3. $\delta^{18}\text{O}$ vs $\delta^2\text{H}$ values of waters from the Australian Alps (data from Table 1) relative to the global meteoric water line (GMWL: Clark and Fritz, 1997) and the Melbourne meteoric water line (MMWL: Hughes and Crawford, 2012). Each data point represents an individual sample collected on the date 15 indicated in Table 1. Error bars are analytical uncertainties (0.2‰ for $\delta^{18}\text{O}$ and 1‰ for $\delta^2\text{H}$). Rainfall samples: B = Mount Buffalo multi-month samples, W = 2 week winter precipitation sample, O = other samples from southeast Australia. Dashed line (slope, $s = 5$) is fit to all of the data by linear regression.

Fig. 4. ${}^3\text{H}$ activities vs $\delta^2\text{H}$ values of waters from the Australian Alps (data from Table 1). Error bars are analytical uncertainties (1‰ for $\delta^2\text{H}$ and ${}^3\text{H}$ from Table 1). Rainfall samples: B = Mount Buffalo multi-month samples, W = 2 week winter precipitation sample, O = other samples from southeast Australia. Linear regression line is fit to the multi-month Mount Buffalo samples. Arrowed lines show changes in 20 ${}^3\text{H}$ activities and $\delta^2\text{H}$ values due to evaporation (Evap) and radioactive decay of ${}^3\text{H}$.

Fig. 5. ${}^3\text{H}$ activities vs. Cl (5a), Na (5b), Si (5e) concentrations and Cl/Br (5c), Na/Cl (5d), Si/Cl (5f) ratios 25 (data from Table 1). Arrowed lines illustrate trends expected from major geochemical processes. Ovens data are from the upper Ovens Valley streams in December 2013 and February 2014 (Cartwright

and Morgenstern, 2015); the geochemistry of these larger streams is similar to the eucalypt forest streams in the Victorian Alps.

Fig. 6a. Comparison of mean transit times from different lumped parameter models, calculated using Eqs 1 to 3 assuming a ${}^3\text{H}$ activity of recharge of 3.0 TU (based on the rainfall samples). DM = Dispersion

5 model with D_p of 0.1 and 1.0; EM = Exponential flow model; EPF = Exponential-piston flow model with

EPM ratio = 0.33 and 1.0. **6b.** Mean transit times from the exponential flow model (EPM = 0.33) with

${}^3\text{H}$ activities of modern recharge ranging from 3.0 to 3.4 TU. Shaded fields show ${}^3\text{H}$ activities in the peatlands waters and eucalyptus forest streams, arrow is the median ${}^3\text{H}$ activity in the peatland waters

(data from Table 1).

10 **Fig. 7.** ${}^3\text{H}$ activities vs. catchment areas for the peatlands and eucalyptus forest catchments. Area error bars assume a $\pm 10\%$ measurement error, ${}^3\text{H}$ error bars are from the analytical uncertainties. Data from Table 1.

Fig. 8. Impact of aggregation on calculated mean transit times. Apparent mean transit times are calculated from the ${}^3\text{H}$ activities of mixtures of waters with actual mean transit times of between 10

15 and 50 years using the exponential-piston flow model with and EPM ratio of 0.33. Actual mean transit times are calculated from the weighted average mean transit times in the mixed water. The binary curve represents variable mixtures of the two end-members, the shaded field represents mixtures of multiple waters with mean transit times of between 10 and 50 years. The red line represents agreement between apparent and actual mean transit times.

Supplementary Material

Fig. S1. Annotated Google Earth® images of Mount Buffalo (Fig. S1a), Falls Creek (Fig. S1b), and Dargo (Fig. S1c) catchments showing extent of the peatlands and the sampled eucalypt forest catchments. Sampling site abbreviations (sites in Table 1). Fig S1a: Cres = Buffalo Cresta, Cry = Buffalo Crystal, BF =
5 Buffalo Forest. Fig. S1b: Cope = Falls Cope, Lan = Falls Langford, Rky = Falls Rocky, FF = Falls Forest. Fig. S1c: D = Dargo, DF = Dargo Forest.

Table 1. Geochemistry of water samples from the Australian Alps

Site ^a	Date	Area ^b	³ H	$\delta^{2}\text{H}$	$\delta^{18}\text{O}$	EC	Na	Mg	K	Ca	Si	Cl	Br	NO_3	SO_4
		km ²	TU	‰ V-SMOW	‰ V-SMOW	$\mu\text{S cm}^{-1}$	mg l ⁻¹								
Peatlands															
<i>Mount Buffalo</i>															
Buffalo Cresta A	26/11/2015	1.5	3.32±0.053	-26	-5.0	19.12	1.12	0.125	0.192	0.621	2.714	0.94	0.0031	0.040	0.072
Buffalo Cresta A	23/02/2015	1.5	2.84±0.058	-41	-7.7	13.72	2.06	0.125	0.168	0.645	2.831	0.95	0.0039	0.048	0.185
Buffalo Cresta B(P) ^b	23/02/2015		2.75±0.055	-41	-7.7	22.33	1.96	0.152	0.273	1.123	3.244	1.08	0.0037	0.285	0.304
Buffalo Cresta C	23/02/2015	2.1	2.75±0.056	-40	-7.5	19.92	1.06	0.121	0.160	0.432	1.632	0.95	0.0036	0.063	0.080
Buffalo Cresta D(P)	26/11/2015		2.70±0.048	-37	-7.3	15.21	1.79	0.131	0.184	0.653	2.601	1.14	0.0038	0.073	0.194
Buffalo Crystal A	23/02/2015	3.5	2.74±0.055	-35	-6.6	12.01	1.97	0.153	0.178	0.684	2.031	1.01	0.0038	0.066	0.207
Buffalo Crystal B	23/02/2015	0.2	2.93±0.058	-30	-5.7	12.65	2.06	0.130	0.250	0.354	3.466	0.99	0.0037	0.320	0.245
<i>Falls Creek</i>															
Falls Cope	24/02/2015	1.9	3.14±0.061	-41	-7.2	9.62	0.92	0.247	0.119	0.519	1.417	0.47	0.0031	0.084	0.076
Falls Langford A	24/02/2015	0.5	3.10±0.060	-39	-7.1	21.42	1.43	0.512	0.203	0.882	2.496	0.64	0.0035	0.250	0.271
Falls Langford B(P)	24/02/2015		2.98±0.059	-43	-8.3	8.52	0.88	0.223	0.160	0.490	0.812	0.70	0.0033	0.165	0.167
Falls Rocky A	24/02/2015	3.5	2.96±0.059	-42	-8.0	7.65	0.79	0.194	0.057	0.463	1.097	0.55	0.0026	0.307	0.111
Falls Rocky A	25/11/2015	3.5	2.90±0.050	-42	-8.1	11.25	0.78	0.149	0.075	0.318	2.103	0.51	0.0018	0.164	0.163
Falls Rocky B(P)	25/11/2015		2.86±0.049	-42	-8.2	7.47	0.62	0.136	0.118	0.255	1.029	0.54	0.0023	0.035	0.130
Falls Rocky C(P)	25/11/2015		3.17±0.055	-35	-6.5	9.54	0.79	0.257	0.245	0.540	1.125	0.51	0.0025	2.097	0.185
Falls Rocky D	25/11/2015	2.6	3.14±0.059	-33	-6.5	16.47	1.04	0.227	0.223	0.403	1.113	0.93	0.0033	0.087	0.079
<i>Dargo</i>															
Dargo A	25/11/2015	5.5	2.84±0.048	-40	-7.7	21.17	1.15	0.930	0.133	1.427	3.259	1.10	0.0040	0.804	0.142
Dargo B	25/11/2015	1.2	2.69±0.043	-43	-8.1	31.9	1.34	1.381	0.334	2.112	2.147	0.91	0.0038	0.493	0.050
Dargo C(P)	25/11/2015		2.47±0.040	-39	-7.0	29.2	1.56	1.667	0.308	1.900	3.012	0.93	0.0038	0.388	0.063
Dargo D	25/11/2015	2.7	3.36±0.053	-35	-6.9	13.9	0.77	0.343	0.097	1.095	2.788	0.83	0.0025	1.845	0.192

<i>Eucalypt Forest</i>																
Buffalo Forest A	24/02/2015	3.3	2.21±0.048	-35	-6.3	42.7	3.89	2.056	0.618	1.727	4.433	1.16	0.0045	0.052	0.740	
Buffalo Forest A	26/11/2015	3.3	2.35±0.042	-34	-6.4	39.5	3.27	1.878	0.470	1.536	4.844	1.30	0.0048	0.038	0.763	
Falls Forest A	24/02/2015	3.3	1.56±0.037	-38	-7.4	65.2	5.70	3.230	0.543	3.686	5.060	2.60	0.0097	0.104	0.499	
Falls Forest B	24/02/2015	1.5	2.10±0.047	-37	-7.5	45.7	3.24	2.092	0.445	2.149	4.233	1.09	0.0045	0.038	0.608	
Falls Forest C	25/11/2015	6.4	2.26±0.040	-31	-6.2	45.3	3.41	1.855	0.566	1.623	6.236	1.20	0.0048	0.418	0.901	
Falls Forest D	25/11/2015	5.8	1.70±0.035	-37	-7.3	56.0	4.78	2.793	0.400	3.092	9.540	1.22	0.0045	0.022	0.581	
Dargo Forest A	25/11/2015	6.1	2.00±0.036	-29	-5.7	44.1	4.12	1.898	0.542	1.654	5.328	1.24	0.0045	0.240	0.408	
<i>Rainfall</i>																
Buffalo	Feb 2015 (12) ^d		2.85±0.057	-36	-7.0	11.58	0.68	0.011	0.058	0.214	0.081	0.98	0.0039	0.015	0.081	
Buffalo	Nov 2015 (9)		2.88±0.051	-35	-6.5	12.20	0.53	0.117	0.108	0.361	0.077	0.80	0.0028	0.106	0.171	
Buffalo	Dec 2013 (17)		2.99±0.046	-38	-7.3		0.87					1.10				
Buffalo	Feb 2014 (2)		2.90±0.049	-37	-7.1											
Buffalo	Jul 2014 (<1)		2.52±0.043	-40	-7.9											
Buffalo	Sep 2014 (3)		2.71±0.044	-34	-6.8											
Melbourne ^e	Jul 2013 (12)		2.72±0.045	-33	-6.3											
Otways ^e	Sep 2014 (6)		2.45±0.041	-22	-4.4											
Latrobe ^e	Aug 2015 (12)		2.76±0.043	-36	-6.8											

Notes: ^a Sampling regions on Fig. 1; ^b Catchment area; ^c P = Piezometer sample; ^d Month collected and number of months represented by the sample; ^e Other rainfall from SE Australia. The rainfall samples represent aggregated samples collected over the number of months indicated, all other samples are individual samples.

Table 2. Calculated mean transit times

Site ^a	Date	Mean Transit Time (yrs)						
LPM ^b		EPF (3.4) ^c	EPF (3.2)	EPF (3.0)	EPF (3.4)	EM (3.4)	DM (3.4)	DM (3.4)
Parameter ^d		0.3	0.3	0.3	1		0.1	1
Peatlands								
<i>Mount Buffalo</i>								
Buffalo Cresta A	26/11/2015	<1	ND ^c	ND	<1	<1	<1	<1
Buffalo Cresta A	23/02/2015	3.4	2.2	1.0	3.3	3.5	2.7	4.0
Buffalo Cresta B(P)	23/02/2015	4.1	2.9	1.6	3.9	4.4	3.9	4.9
Buffalo Cresta C	23/02/2015	4.1	2.9	1.6	3.9	4.4	3.9	4.9
Buffalo Cresta D(P)	26/11/2015	4.4	3.2	1.9	4.2	4.8	4.2	5.4
Buffalo Crystal A	23/02/2015	4.2	3.0	1.7	3.9	4.4	3.9	5.3
Buffalo Crystal B	23/02/2015	2.8	1.6	<1	2.7	2.9	2.8	3.3
<i>Falls Creek</i>								
Falls Cope	24/02/2015	1.4	<1	ND	1.4	1.5	1.4	1.5
Falls Langford A	24/02/2015	1.7	<1	ND	1.7	1.7	1.7	1.9
Falls Langford B(P)	24/02/2015	2.4	1.3	<1	2.4	2.5	2.4	2.9
Falls Rocky A	24/02/2015	2.6	1.4	<1	2.5	2.7	2.5	3.0
Falls Rocky A	25/11/2015	3.0	1.8	<1	2.9	3.1	2.9	3.5
Falls Rocky B(P)	25/11/2015	3.3	2.1	<1	3.2	3.5	3.2	3.9
Falls Rocky C(P)	25/11/2015	1.3	<1	ND	1.3	1.3	1.3	1.4
Falls Rocky D	25/11/2015	1.4	<1	ND	1.4	1.5	1.4	1.5
<i>Dargo</i>								
Dargo A	25/11/2015	3.4	2.2	1.0	3.3	3.6	3.2	4.0
Dargo B	25/11/2015	4.5	3.3	2.0	4.3	4.9	4.3	5.6
5.2Dargo C(P)	25/11/2015	6.5	5.4	4.0	6.0	7.4	6.0	8.0

Dargo D	25/11/2015	<1	ND	ND	<1	<1	<1	<1
<i>Eucalypt Forest</i>								
Falls Forest A	24/02/2015	28.9	28.8	28.6	26.0	39.0	37.2	40.2
Falls Forest B	24/02/2015	11.5	10.8	9.6	9.9	16.4	10.0	17.7
Buffalo Forest A	24/02/2015	9.7	8.8	7.5	8.7	13.0	8.6	14.7
Falls Forest C	25/11/2015	9.1	8.1	6.6	8.0	11.3	7.9	13.2
Falls Forest D	25/11/2015	22.6	22.2	21.6	17.2	30.7	16.7	31.4
Dargo Forest A	25/11/2015	14.0	12.4	11.2	11.3	18.8	11.1	19.6
Buffalo Forest A	26/11/2015	7.8	6.9	5.3	7.0	9.4	7.0	10.8

^a Sites on Fig. 1 as Supplementary Figure S1

^b Lumped parameter model (DM = Dispersion model; EM = Exponential flow model; EPF = Exponential-piston flow

model) ^c Assumed ³H activity of modern recharge in brackets

^d EPM or D_p parameter

^e Not determined as ³H activity higher than assumed value of recharge

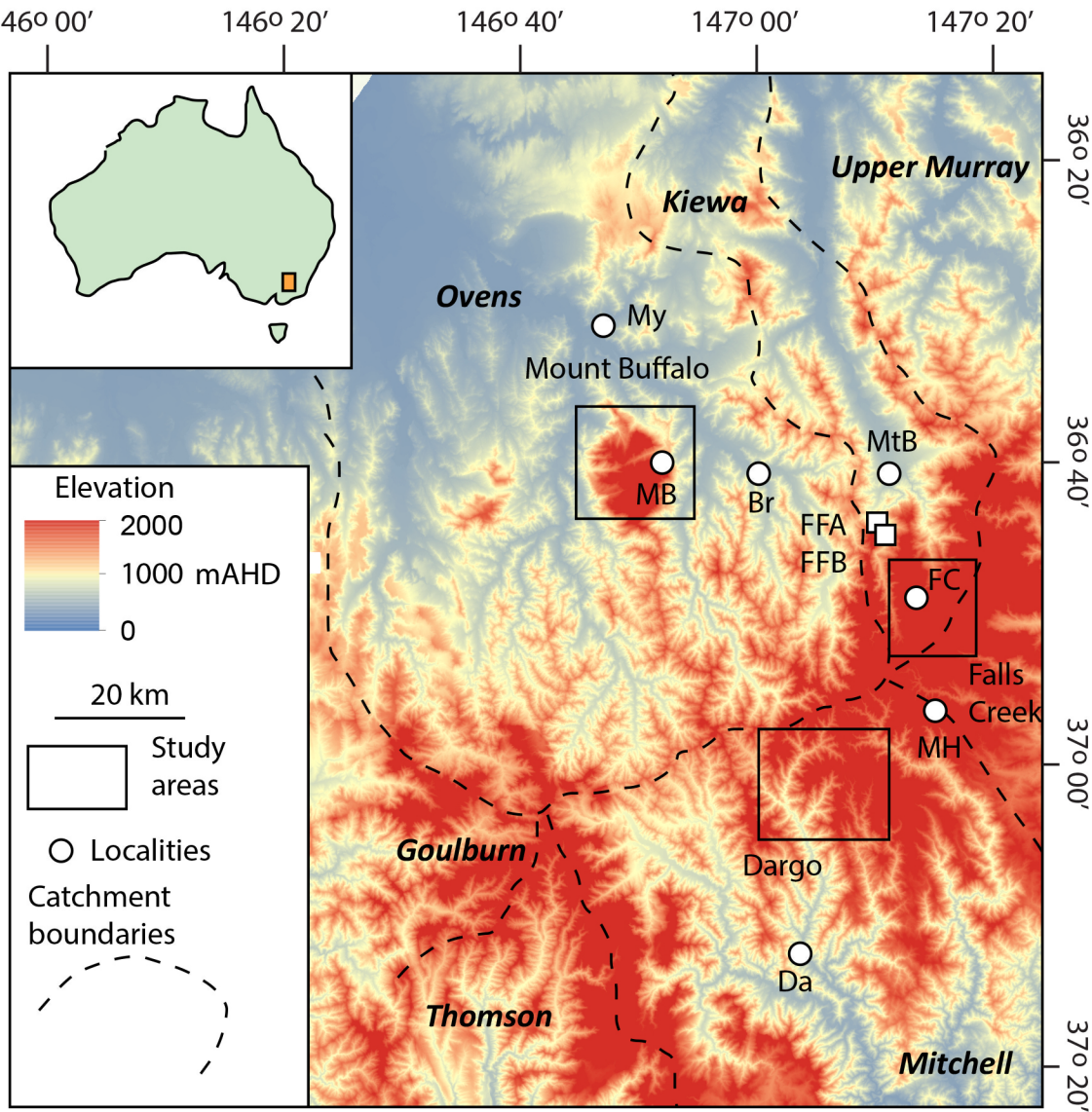
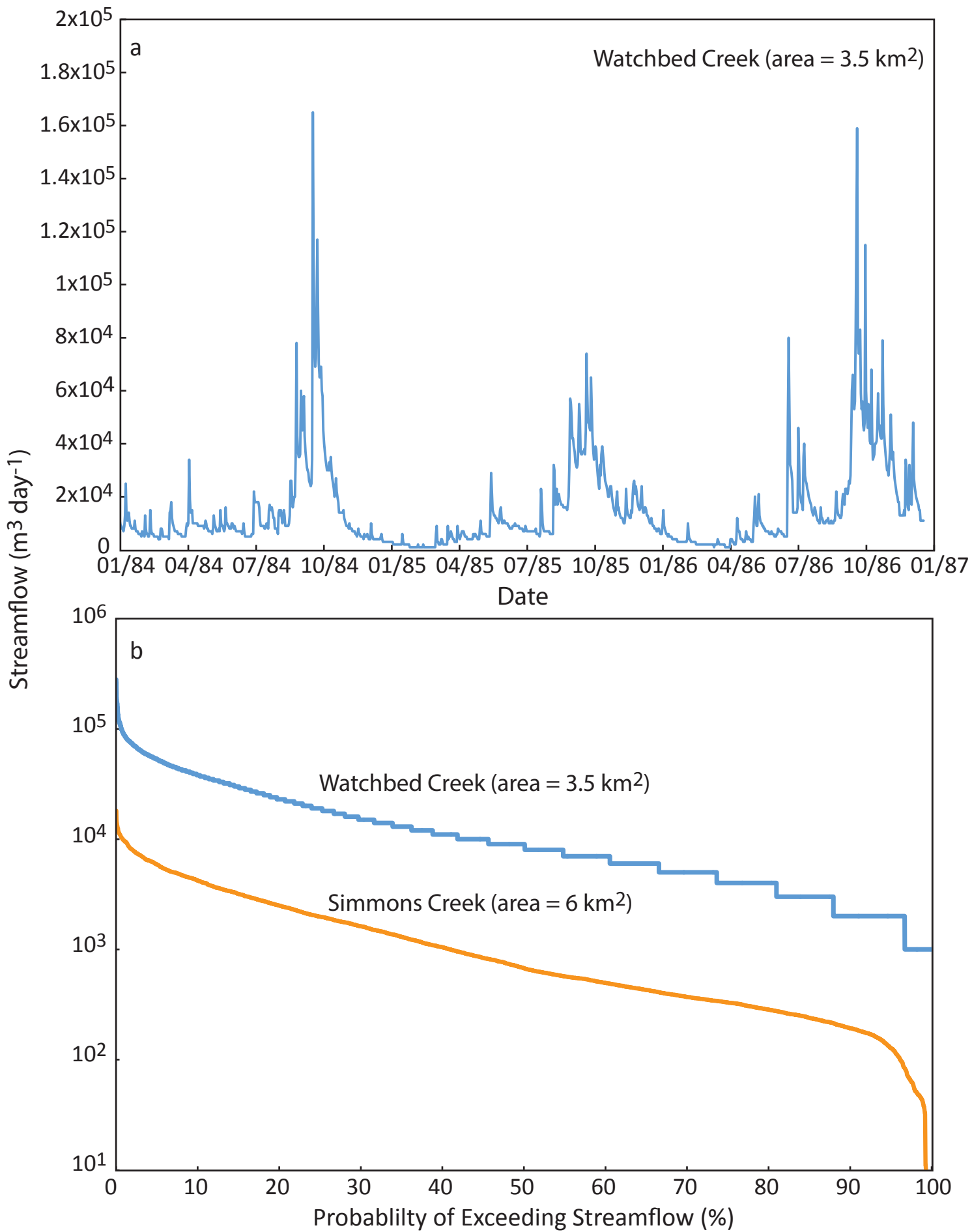
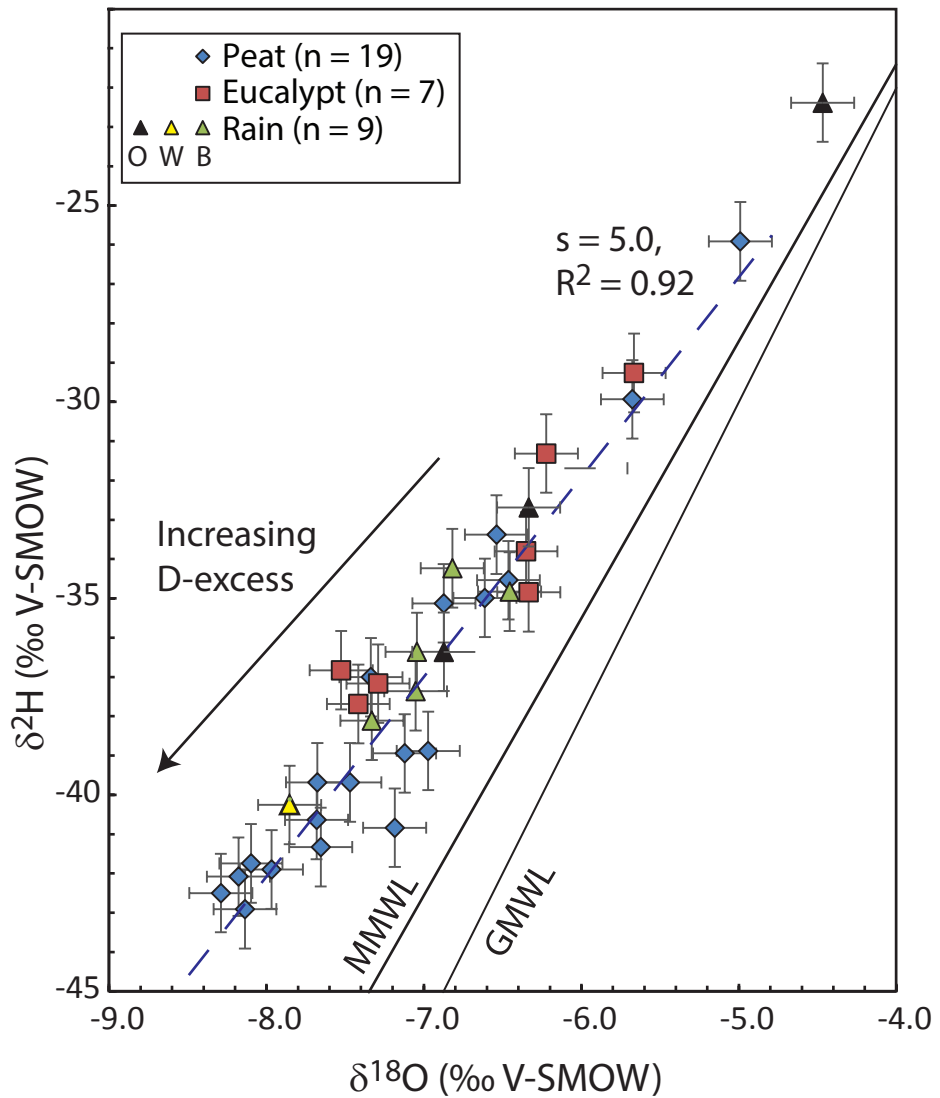
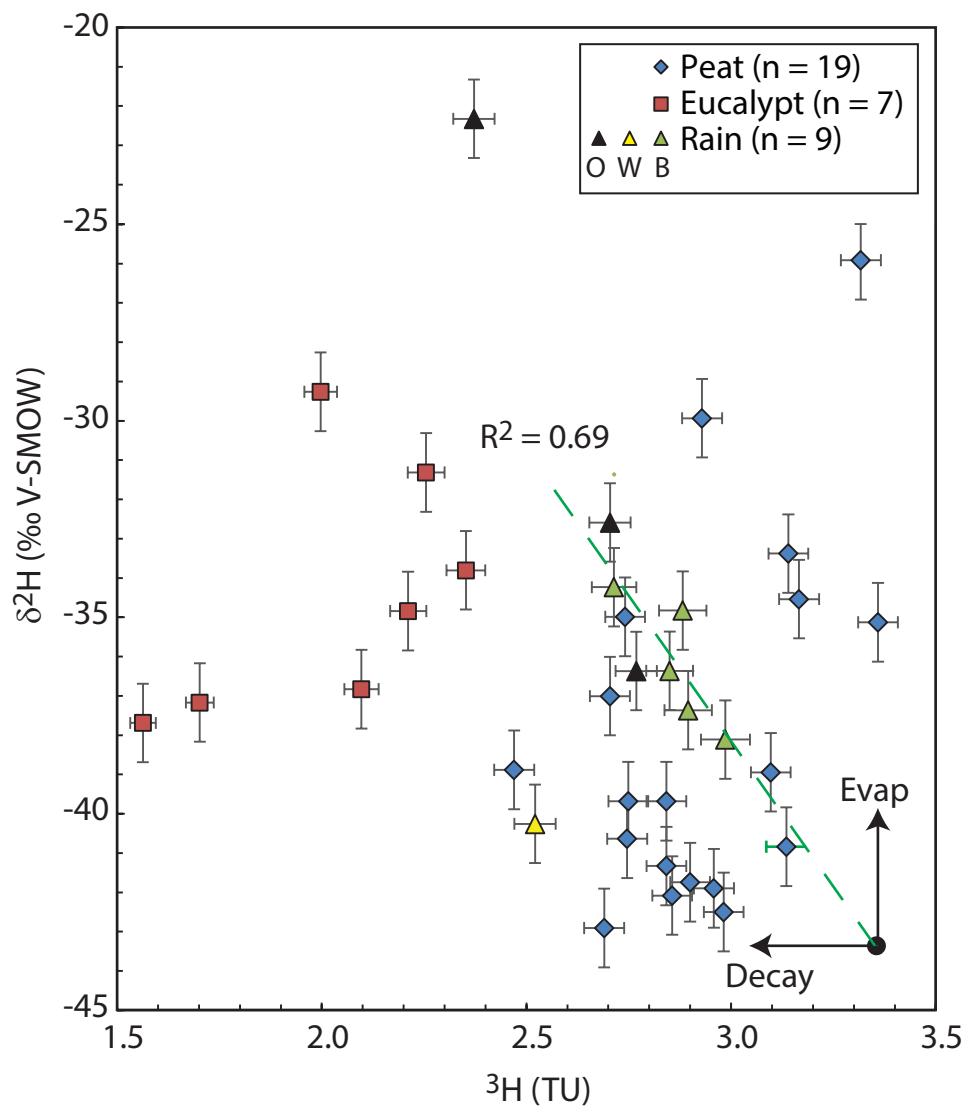
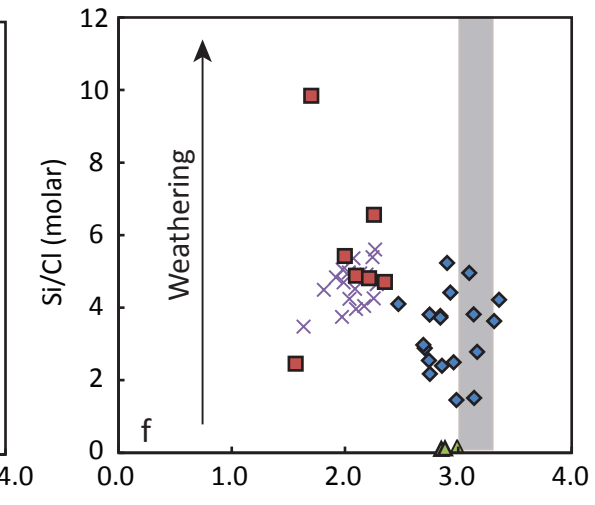
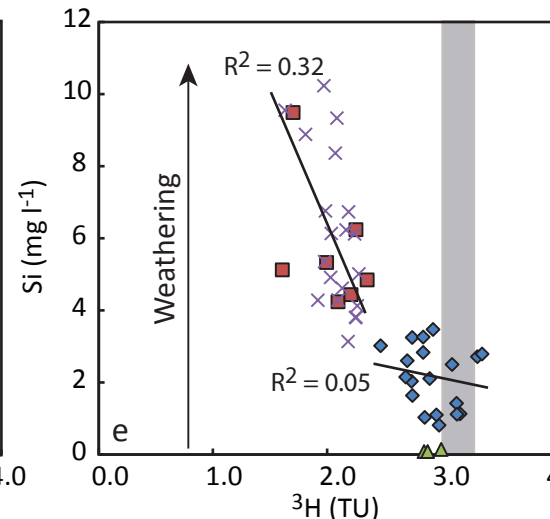
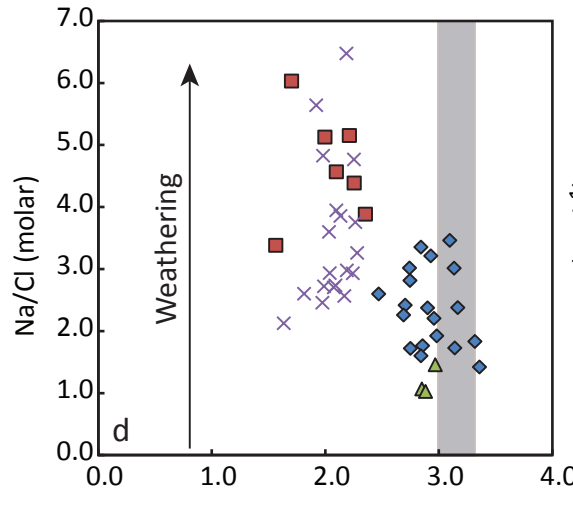
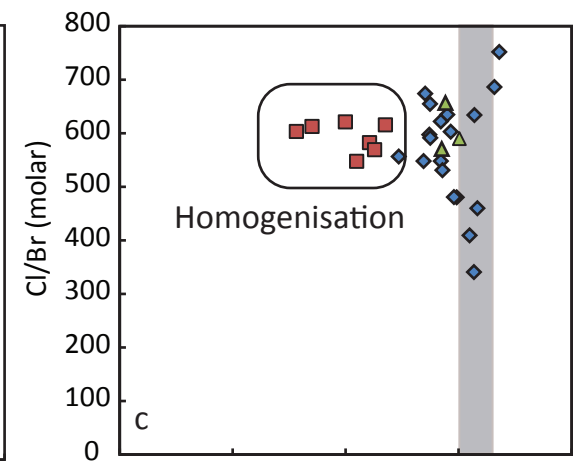
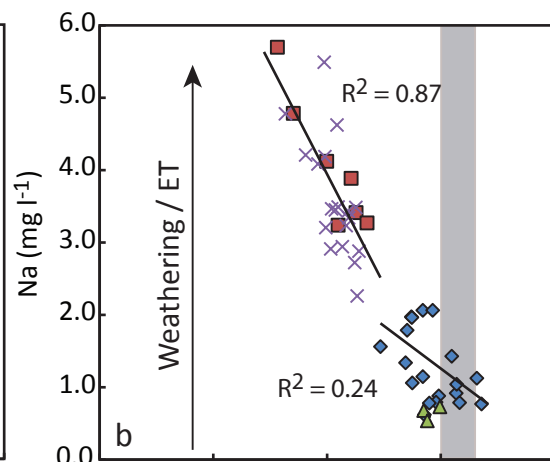
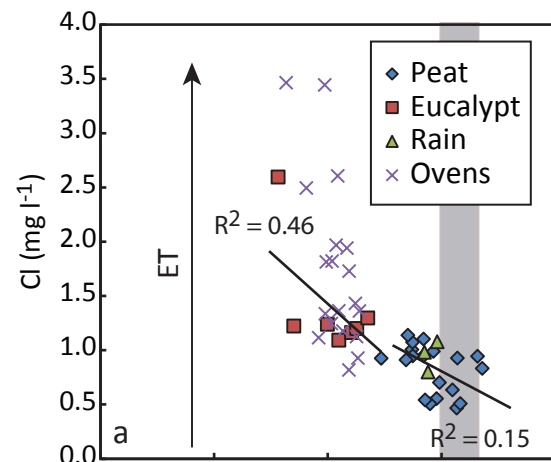


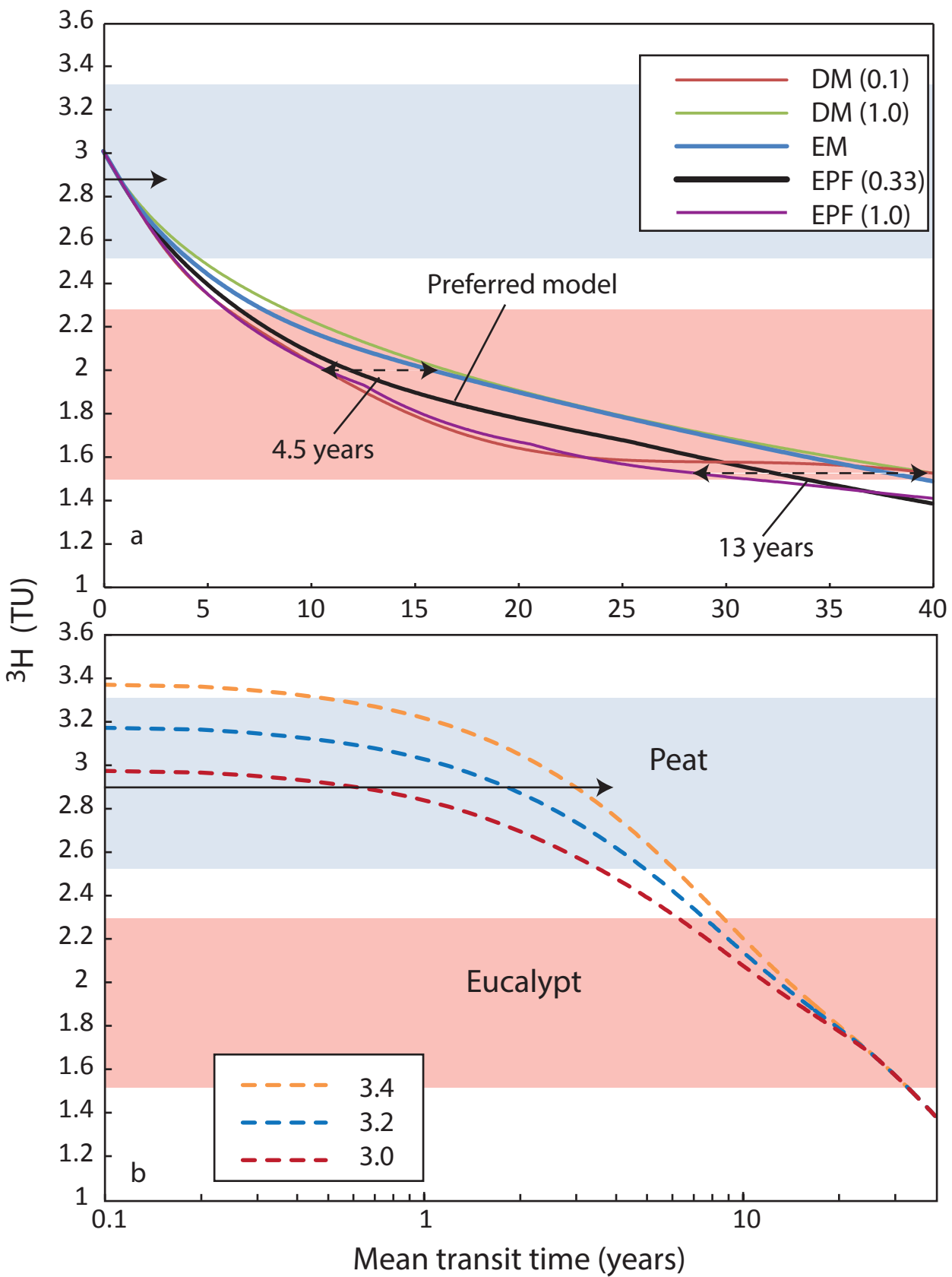
Fig. 2











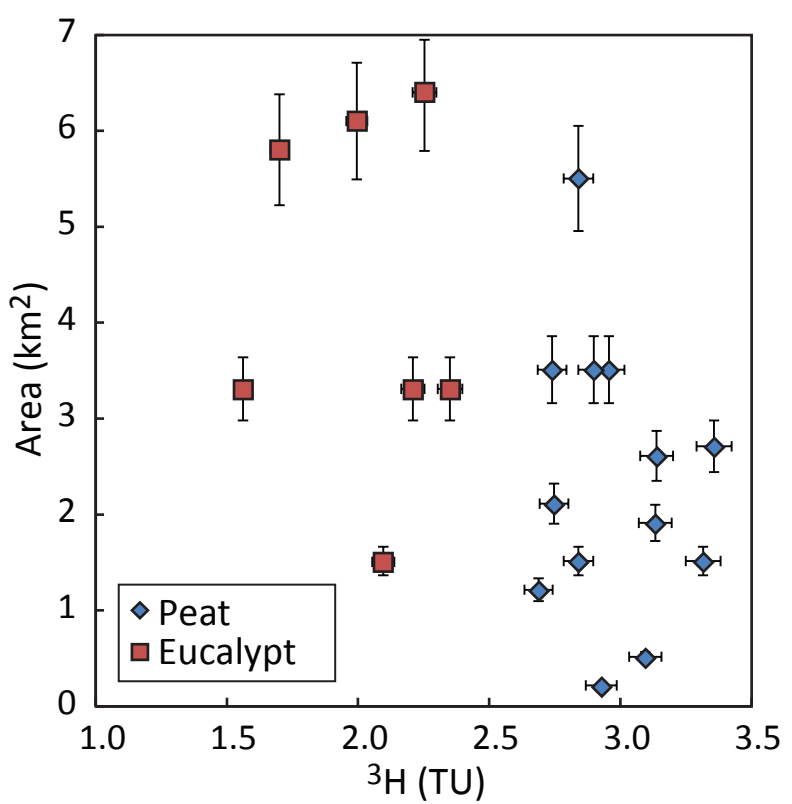


Fig. 8

